SLAC-PUB-2231
November 1978
(T/E)

CHARM AND TAU MEASUREMENTS FROM DELCO[1*]

Jasper Kirkby
Stanford University

I. INTRODUCTION

DELCO has just completed its data-taking period of eighteen calendar months at SPEAR. The detector has distinguished itself from other '4π' spectrometers by emphasizing clean electron identification over a broad energy range at the expense of poorer momentum resolution. This characteristic allows a general purpose probe of both charm and τ decays via the transitions $c \to s\, e^+ \nu_e$ and $\tau^- \to \nu_\tau\, e^- \bar{\nu}_e$ respectively. Both decays have the merit of large ($\geq 10\%$) branching ratios and consequently we have accumulated relatively strong data samples (1K eX events from τ decays and 5K multiprong electron events from charm and τ decays).

Most of our analysis so far has emphasized τ studies (which are discussed in section V). However, I will also show you what we know from cross sectional measurements (section III) and from preliminary studies of D semileptonic decays at the ψ'' (section IV). There will be very little discussion of the interesting subject of di-electron events (2 electrons + $\geq$ 1 charged particle $\neq$ e) since our analysis is in an early stage.

Finally, I refer the reader to the excellent series of lectures by Stanley Wojcicki at this Summer Institute. These contain both a general discussion of how our measurements fit into the overall picture of weak decays and a far more thorough list of references on this broad subject. As a result I can, and will, primarily concentrate on simply presenting the experimental data.

*Work supported in part by the U.S. National Science Foundation and in part by the Department of Energy under contract EY-76-C-03-0515.

Presented at the Summer Institute on Particle Physics, Weak Interactions Present and Future, Stanford, Ca., July 12 - 21, 1978.

II. APPARATUS

The apparatus (Figs. 1a) and 1b)) consists of a tracking system of cylindrical multiwire proportional chamber and planar magnetostrictive wire spark chambers (WSC) separated by a one-atmosphere ethane threshold Cerenkov counter. The latter provides clean electron identification ($P_{\pi \to e} < 10^{-3}$) down to a momentum of 0.2 GeV (below which the Cerenkov light images are displaced off the phototubes). A magnet provides an analyzing field integral of 1.7 kG-m which results in a momentum accuracy of $\sigma_p/P = 8P$ (GeV)% due to measurement errors and 5.2% due to multiple Coulomb scattering. The outer-most detector layers are an array of Pb/scintillator shower counters which cover 60% of 4π steradians and a pair of Pb walls, followed by scintillation counters and WSC, which allow π/μ separation over 20% of 4π steradians.

III. THE R AND R_e PLOTS

A. Hadronic Cross-Section

Historically the R plot has been the single most fruitful measurement made in e^+e^- annihilations. (R is defined by $R = \sigma(e^+e^- \to \text{hadrons})/\sigma(e^+e^- \to \mu^+\mu^-)$ and its variation is measured with centre-of-mass energy.) It was the first indicator of a new flavour, charm, it supports the colour hypothesis and measures the quark charges, it revealed an extra contribution due to the τ lepton and led to the spectacular observations of the ψ and ψ'.

For the last couple of years or so it has been used as a R(oad) map to lead experimentalists to productive centre-of-mass energies. The most notable success has been the ψ''[2] which is found just above charm threshold at E_{CM}=3.77 GeV. At this energy 30% of the hadronic events are due to

pure $D\bar{D}$ initial states (roughly half $D^0\bar{D}^0$). Furthermore the D's have a low velocity ($\beta\sim0.14$) so there are rather small differences between LAB and CM quantities. The studies of D semi-leptonic decays discussed in Section IV were made at this resonance.

The value of R in the range $3.50 < E_{CM} < 4.8$ GeV, after removal of the ψ and ψ' radiative tails, is shown in Fig. 2. No further radiative corrections have been applied to these data since they exagerate fluctuations which may be both statistical and authentic. This in turn leads to difficulties in identifying resonances and in making comparisons with other experiments.

The hadronic detection efficiency has been determined from the observed prong and photon distributions and is $0.85^{+0.05}_{-0.10}$ over this range. The bars indicate only statistical errors and thereby do not reflect an overall systematic error of ±15% due to model uncertainties, event losses and backgrounds such as those due to beam gas scattering. Any variation in systematic erros vs. E_{CM} is smooth and so the statistical error bars are appropriate indicators of structure.

The value of R below charm and τ thresholds at E_{CM}=3.50 and 3.52 is $2.0 \pm 0.1 \pm 0.3$ [3] in good agreement with the coloured quark prediction of $3(Q_u^2 + Q_d^2 + Q_s^2) = 2$. The dashed line in Fig. 2 represents the constant contribution from 'old physics' at higher energies.

Beyond the resonance region, R again assumes an approximately constant energy dependence with the new value $4.4 \pm 0.2 \pm 0.6$. From our τ measurements we determine a contribution (indicated by the dot-dashed line) of 0.85 ± 0.15 to this increase and thereby infer a residue due to charm of $4.4 - 2.0$ (old physics) $- 0.85(\tau) = 1.55 \pm 0.2 \pm 0.2$. Once more

this is compatible with the quark model prediction of 4/3.

The residual charm component of the hadronic cross section (R^c) is shown in Fig. 3. The data display considerable structure: sharp rises just above thresholds for production of $D\bar{D}$ (centered at 3.77 GeV), $D\bar{D}^*$ (3.92 GeV) and $D^*\bar{D}^*$ (4.03 GeV) and a sharp dip at E_{CM} = 4.25 GeV. The region between 4.03 and 4.2 GeV is reasonably flat and the 4.4 GeV peak is rather modest in contrast with the observations[4] of other experiments (Fig. 4). Part of these discrepancies is due to the afore-mentioned application of radiative corrections. The theoretical models for these structures include both s-channel poles due to a $c\bar{c}$ state[5] (charmonium) and bound states of two quarks and two anti-quarks[6] ($D\bar{D}$ molecules).

B. Multi-Prong Electronic Cross-Section

Both the τ and the lightest charmed particles will give rise to 'prompt' single electrons since they have weak-decay lifetimes ($\sim$few 10^{-13}sec) which are much shorter than those familiar from kaon decay ($\sim 10^{-8}$sec). Since electromagnetic sources produce electrons in pairs, which can thereby be identified and rejected, the study of inclusive electron production provides a sensitive technique for observing the new particles.

The inclusive electron cross section is expressed as $R_e = \sigma(e^+e^- \to e^\pm + \geq 2 \text{ charged particles})/\sigma(e^+e^- \to \mu^+\mu^-)$. The variation of this quantity in the range $3.5 < E_{CM} < 4.8$ GeV is shown in Fig. 5. Events containing two or more prompt electrons have been excluded from these data. A prompt electron is identified as a single track which appears to originate from the interaction region and possesses in-time Cerenkov and shower counter pulses. The minimum pulse heights correspond to 0.7 photo-electrons for the Cerenkov counter and 0.3 minimum ionizing particles for the shower counter.

The track is required to have at least one hit in either the first (innermost) or second cylindrical proportional chambers in order to decrease photon conversion backgrounds.

We will now discuss the backgrounds to these data. The dominant electron source is pair production both by externally and internally converted photons from π^o decay. We can estimate this background assuming 3 π^o's per hadronic event and a 1% beam-pipe radiator. The number of external γ conversions per hadronic event is $\sim$ 6x .01 x 0.5(Ω) $\sim$ 0.03 which is approximately equal to the charm signal rate $\sim$(1.3/5)x2x0.1x0.5$\sim$0.03 per hadronic event (assuming a semileptonic branching ratio of 0.1). Most Dalitz pairs and photons which convert in the beam pipe are removed by requiring that the candidate electrons are unaccompanied by another track of opposite charge and small relative ('opening') angle. A fake signal is also generated by the spatial coincidence of a charged track with a photon conversion in the 'blind' region at the entrance to the Cerenkov counter or in the ethane radiator itself. We measure this process to occur at the level $(4.2\pm0.3)10^{-3}$ per hadronic event and have applied this correction to Fig. 5. The probability for a non-electron to be detected by the Cerenkov counter is $(0.8\pm0.3)10^{-3}$, as determined from $\mu^+\mu^-$ events. This is consistent with the production rate of δ rays above the electron Cerenkov threshold in ethane (14 MeV). This background is very small (<3% of the charm signal) since the majority of the pion momenta are below 500 MeV/c and thereby cannot give rise to δ rays exceeding 14 MeV.

After removal of these backgrounds, the value of R_e at E_{CM}=3.50, 3.52 GeV is 0.03±0.01 which represents the residue from unsubtracted backgrounds such as asymetric Dalitz decays and two-photon electron production. Until we have a better understanding of the nature of this residual background

we will naively assume it has a constant energy dependence as indicated by the dashed line. Above the τ and D thresholds the data exhibit a striking increase and a structure similar to the hadronic production. These data contain a large contribution from τ decays (dot-dashed-line) according to measurements described in Section V.

It is instructive to compare quantitatively the electron production from charm R_e^c (Fig. 6) with the total charm cross section (Fig. 3). This comparison is made by plotting the ratio R_e^c/R^c (Fig. 7). The value at E_{CM}=3.77 GeV provides a direct measurement of the semileptonic branching ratio, b_e^D, averaged over an equal flux of D^o and D^+. In a 4 MeV energy range which is centred on the ψ", we find $R^c = 0.97 \pm 0.02$ and $R_e^c = 0.192 \pm 0.021$, where the quoted errors are statistical and events involving two detected electrons are excluded. We therefore measure,

$$2b_e^D\,(1-0.25\,b_e^D) = R_e^c/R^c = 0.20 \pm 0.023$$

$$\text{i.e.} \qquad b_e^D = 0.10 \pm 0.02.$$

The final result includes an estimation of systematic errors.

The data of Fig. 7 display, within systematic errors, a constant or perhaps slightly falling electron contribution from charm. It is especially interesting to note that electron production at the energies 4.16 and 4.4 GeV, which are associated with F production, shows no significant departure from the D regions. This implies either a small F cross-section or semileptonic branching ratio similar to the D.

C. Two-Electron Multiprong Cross Section

Events which contain two prompt electrons in addition to hadrons cannot arise from the decay of a sequential heavy lepton pair but will be generated by the simultaneous semi-leptonic decays of a pair of charmed particles. As such they provide good sensitivity to certain features of the charm semileptonic decays despite a statistical reduction by a factor of 20 relative to

the one-electron events.

The important backgrounds are π^o Dalitz decays, the cascade decays $\psi' \to X\,\psi \to e^+e^-$ and electrons from the two-photon process. These are inhibited by the requirements that the e^+e^- pair mass exceed 135 MeV/c^2, the coplanarity angle $\phi_{ee} < 160^o$ and that at least one non-electron track is present with a momentum above 200 MeV/c and with a polar angle $55^o < \theta < 125^o$.

After applying these restrictions there remain 75 events in the range $3.1 < E_{CM} < 4.25$ (ψ' excluded). The cross section $R_{2e} = \sigma(e^+e^- \to e^+e^- + \geq 1$ prong $\neq e)/\sigma(e^+e^- \to \mu^+\mu^-)$ is shown in Fig. 8. We have arbitrarily allowed the rate in the range $3.5 < E_{CM} < 3.67$ GeV to define the background level.

The data are consistent with the charm production energy-dependence we saw earlier. At the ψ'' we measure,

$$R_{2_e}/R^c = (b_e^D)^2 = 0.015 \pm 0.005$$

or,
$$b_e^D = 0.12 \pm 0.02 \pm 0.04$$

where the second (systematic) error reflects model uncertainties. For example, if the dominant decay mode is $D \to Ke\nu$ then the acceptance of D^+D^- events is almost a factor of two lower than $D^o\bar{D}^o$ events. (This follows from the poor detection efficiency of neutral kaons.) The data of Fig. 8 assume equal contributions from $D^o\bar{D}^o$ and D^+D^- events and equal $Ke\nu$ and $K^*e\nu$ partial rates; if we make the extreme assumption that only D^+D^- events contribute then $b_e^+ = 0.14 \pm 0.02 \pm 0.04$.

This measurement can be used to set limits on the separate D^+ and D^o semileptonic branching ratios (b_e^+ and b_e^o, respectively). For example, in the extreme case that $b_e^+ \sim 20\%$ and $b_e^o \sim 0\%$, the one-electron data at the ψ'' would lead to a measurement $b_e^D = 10\%$. However we would observe an anomalously large (by a factor of two) di-electron yield since this is proportional to

$(b_e^+)^2 + (b_e^o)^2$. Unfortunately, the present errors in R_{2e} do not allow a useful measurement.

The presence of a charm-changing neutral current would result in the decay $D \to e^+e^-X$. The two-electron cross section therefore measures,

$$(b_e^D)^2 + 2\, b_{ee}^D = R_{2e}/R^c$$

where b_{ee}^D is the branching ratio for $D \to e^+e^-X$ and we assume equal D^o and D^+ semileptonic branching ratios (given by $b_e^D = 0.10 \pm 0.02$). At the ψ'' we find,

$$(.10 \pm .02)^2 + 2\, b_{ee}^D = .015 \pm .005$$

or,

$$b_{ee}^D < 0.008 \text{ (95\% CL)}.$$

This measurement is an order-of-magnitude weaker than the limit determined by the Columbia-BNL group from the ratio $\mu^- e^+ e^- / \mu^- e^+$ from ν_μ interactions in the FNAL 15' bubble chamber.[7)]

IV. D SEMI-LEPTONIC DECAYS

A. Electron Spectrum

Since the basic charmed quark electronic decay is $c \to s\, e^+ \nu_e$ we expect the following channels to contribute to the semi-leptonic decays of D mesons:[8)9)]

$$D \to K e\nu$$

$$D \to K^*(890)\, e\nu$$

$$D \to K^{**}(1420)\, e\nu$$

$$D \to Q\,(1290)\, e\nu$$

$$D \to K\,(n\pi)\, e\nu$$

The decays are unlikely to contain three kaons due to phase-space suppression. This argument also applies to $K^{**}(1420)$ and Q(1290). The decays to $K(n\pi)$ with n larger than 2 or so are not only suppressed by the available phase space but also by the low energy theorem which says that the semileptonic decay rate vanishes if any one of the pions is soft.[8] The anticipated D semileptonic decays are therefore $D \to Ke\nu$, $K^*e\nu$ and $K(n\pi)e\nu$ ($n \leq 2$), with some prejudice that the $K\pi$ channel is dominated by the K^* pole.

In addition there will be smaller contributions from the Cabibbo-suppressed modes:

$$D \to \pi e\nu$$
$$D \to \rho e\nu$$
$$D \to A_1\ e\nu$$

Of these only the $\pi e\nu$ mode may be significant since, in contrast with the other decays, it benefits from a modest phase-space enhancement so that,

$$\frac{\Gamma\ (D \to \pi e\nu)}{\Gamma\ (D \to Ke\nu)} = 1.6\ \tan^2\theta_c$$

where θ_c is the Cabibbo angle.

The most direct experimental quantity which distinguishes between the various semi-leptonic decays is the electron momentum spectrum. The effect of decay to a higher-mass hadronic state is of course to soften the electron momenta (as illustrated in Fig. 9).

The electron spectrum obtained in the multiprong events at the ψ'' (Fig. 10) must be corrected for backgrounds before it can provide information about the D decays. The τ background (dot-dashed line) is well-determined and is the predominant source of high-energy electrons. The residual hadronic background spectrum (dashed line) has been determined from data taken in the energy range $3.50 < E_{CM} < 3.67$ GeV (after removal of the τ electrons) and from hadronic events at the ψ''. The final spectrum

after removal of these backgrounds is shown in Fig. 11.

We will use these data to determine the relative contributions from $K^*e\nu$ and $Ke\nu$ on the assumption that these are the dominant semi-leptonic decay modes. The results of the fit (which includes a fixed $\pi e\nu$: $Ke\nu$ fraction of 1.6 $\tan^2\theta_c$) are illustrated in Fig. 11 and provide the following measurements:

$$\Gamma(D \to Ke\nu)/\Gamma(D \to Xe\nu) = 0.37 \pm 0.20$$

and, $$\Gamma(D \to K^*e\nu)/\Gamma(D \to Xe\nu) = 0.60 \pm 0.20$$

where the errors include an estimate of systematic effects. Under the assumption that the major semi-leptonic decays are $K^*e\nu$ and $Ke\nu$ we therefore measure the branching ratios,

$$BR\ (D \to Ke\nu) = (3.7 \pm 2.1)\%$$

and, $$BR\ (D \to K^*e\nu) = (6.0 \pm 2.3)\%$$

These errors are, of course, highly correlated.

In a separate fit we have varied the $\pi e\nu$ fraction while holding the $K^*e\nu$: $Ke\nu$ ratio equal to 0.60:0.37. This sets a limit,

$$\Gamma(D \to \pi e\nu)/\Gamma(D \to Xe\nu) < 0.20\ (95\%\ CL)$$

or, $$BR\ (D \to \pi e\nu) < 2.0\%\ (95\%\ CL)$$

B. D Lifetime

We may combine the results obtained from the branching ratio determinations and the electron spectra to measure the lifetime of the D mesons.

As input we need a theoretical calculation of the $\Gamma(D \to Ke\nu)$[8)9)]. This decay can be fairly rigorously calculated in contrast with purely hadronic channels, as demonstrated by the successful analogous treatment applied to K_{e3} and $K_{\mu 3}$ decays. The result is $\Gamma(D \to Ke\nu) = (1.4 \pm 0.3)$ $10^{11}\,sec^{-1}$ where the error reflects form factor uncertainties.

If we make the assumption that the D^o and D^+ lifetimes (τ_D) are equal then by combining this theoretical calculation with our experimental branching ratio measurement we find,

$$\tau_D = (0.037 \pm 0.021)/((1.4 \pm 0.3)\ 10^{11})$$
$$= (2.6 \pm 1.5)\ 10^{-13}\ \text{sec}$$

However, it may be invalid to assume that the hadronic decay rate of the D^o and the D^+ are equal since the D^o can decay to both I=1/2 and 3/2 final states whereas the D^+ can decay only to I=3/2 states. The conjecture of several authors[10] in fact is that $\Gamma(D^+ \to \text{all}) << \Gamma(D^o \to \text{all})$. Since the semi-leptonic decay rates of both the D^+ and D^o must be equal we may test this hypothesis by measuring the separate semi-leptonic branching ratios.

An alternative technique to that involving the two electron events is to compare single electron production at the ψ'' and in the range $4.0 < E_{CM} < 4.2$. At each centre-of-mass energy we write,

$$R^o\ b_e^o + R^+\ b_e^+ = R_e$$

where R^o and R^+ are, respectively, the D^o and D^+ cross sections. In principle therefore, the separate semi-leptonic branching ratios may be determined if R^o, R^+ and R_e are known at two centre-of-mass energies which involve different relative amounts of D^o and D^+. This is the case for E_{CM}=3.77 and 4.03 GeV and the measurements are summarized in Table 1 Here we have used Mk I data[11] for the relative D^o:D^+ production at E_{CM}=4.03 GeV and our absolute cross-section measurements in order to provide cancellation of some systematic errors.

Table 1

Input Data Used to Determine the D^o and D^+ Semileptonic Branching Ratios

E_{CM}(GeV)	R^o	R^+	R_e^c
3.77	1.08 ± 0.14	0.86 ± 0.14	0.192 ± 0.21
4.03	2.92 ± 0.36	1.14 ± 0.36	0.399 ± 0.64

The results are,

$$b_e^o = 0.10 \pm 0.05$$

$$\text{and} \quad b_e^+ = 0.10 \pm 0.08$$

The values are very sensitive to input assumptions and the errors are highly correlated. Clearly at present the data are unable to test the hypothesis that the D^+ and D^o lifetimes are different. This conclusion may be reversed after a more careful analysis has been completed on both these measurements and the detailed characteristics of the two-electron events.

C. $D^o\overline{D^o}$ Mixing

In analogy with the K^o-$\overline{K^o}$ system, it is expected that the D^o and $\overline{D^o}$ can transform into one another via intermediate states. However since these states must have zero strangeness the process is inhibited by $\tan^4\theta_c$ ($\sim 10^{-3}$) and the mixing will be negligible within the short D^o lifetime.[12] On the other hand, complete mixing occurs if $|\Delta C|=2$ neutral currents exist at the level of $\gtrsim 10^{-3}$ of the normal weak coupling. A consequence of mixing is the observation of like-sign di-electron events resulting from the process,

$$e^+e^- \to X\, D^o, \overline{D^o} \longrightarrow D^o \longrightarrow X e^+ \nu_e$$
$$\qquad\qquad\quad \hookrightarrow X\, e^+ \nu_e$$

In the D region ($3.72 < E_{CM} < 4.14$ GeV) we observe 46 two-electron events which satisfy the cuts described earlier. Of these, 1 event has like-sign electrons. In the background region, below charm threshold, we observe 7 events of which 2 are like-sign. After adjusting for the relative luminosities we find the single like-sign event in the charm region is consistent with background. On the assumption that half of the observed

electrons are produced by neutral D decay we find,

$$\text{Probability } (D^0 \to \overline{D^0}) < 0.05 \text{ (90\% CL)}$$

V. τ DECAYS

A. Cross Sections

Since a large fraction (70%) of τ decays involve only one-charged particle, they have primarily been studied by means of the anomalous two-prong lepton events, eμ, eX and μX. In our case we have isolated a sample of eX (X≠e) events which have survived certain requirements in order to remove backgrounds. The most important of these are that the X particle does not possess either a Cerenkov tag or a large shower counter pulse-height and that both tracks are acoplanar by at least 20^o. (The acoplanarity angle is defined as the angle between the two planes containing a track and the beam axis). A minimum momentum of 0.3 GeV/c is allowed for the X particle and 0.2 GeV/c for the electron in order to ensure efficient Cerenkov detection. These cuts result in a very clean sample of τ events: the background from misidentified radiative e^+e^- events is about 4% and the charm contamination is <5%, averaged over the full energy range.

The production cross section ratios, $R_{ex}^{2p} = \left(\sigma(e^+e^- \to eX)/\sigma(e^+e^- \to \mu^+\mu^-)\right)$ for eX events with no detected photons are shown in Fig. 12a) and for all eX events in Fig. 12b). The data exhibit a sharp rise at threshold followed by a smooth increase up to a constant high-energy value. This is precisely the energy dependence expected from leptonic pair-production and is in striking contrast with the multi-prong electron data (Fig. 5) which characterizes a charmed hadronic origin.

The fitted curves indicate the (radiatively-corrected) cross section expected for a spin 1/2 τ lepton superimposed on a constant background term. The latter predicts a background of (5±3)% due to particle misidentification in agreement with an independent shower counter pulse height study.

The shape of the anomalous two-prong lepton cross-section has been a corner-stone in the argument for the existence of the τ lepton. These data have been statistically limited until the past year and, given the proximity of the charm and two-prong lepton cross sections, the τ was not considered to be completely established. The remaining doubts were eliminated by the observation[13] of eX events below charm threshold ($E_{CM} = 2M_{D^o} = 3726.6 \pm 1.8$ MeV) An expanded view of the threshold behaviour of the eX events (Fig. 13) clearly distinguishes them from charm.

The data of Fig. 13 are sufficient to exclude all τ spin asignments other than J=1/2.[14] The solid line indicates a spin 1/2 fit after accounting for radiative corrections. These have the effect of reducing the annihilation centre-of-mass energy and thereby decreasing the cross-section (to a level which may reach zero for the collisions which suffer large radiative losses.). If these data result from a pair of integer spin particles then they must be produced in a relative p-state since a boson and its anti-particle have the same parity. The resultant gentle increase in cross section at threshold is in contradiction with observation. (An example of a pair of spin 1 particles is indicated by the dashed line.) However the data are well fit by the steep s-wave threshold resulting from half-integer spins. Spins other than J=1/2 are excluded since they lead to divergent high energy behaviour (an example, J=3/2, is illustrated by the dot-dashed line).

We have determined the precise threshold energy by fitting a radiatively-corrected spin 1/2 curve and constant background term to the data of Fig. 12b). The χ^2 variation of this fit vs. threshold beam energy (Fig. 14) measures the τ mass as,

$$m_\tau = 1782^{+3}_{-4} \quad \text{MeV}/c^2$$

Although the two-prong electron data is relatively free of charm at all energies the same is certainly not true of the multi-prong electron data (Fig. 5). However there is a brief window between the τ and charm thresholds where we can observe any τ decay with zero charm contamination. The τ cross-section is rather small ($R_{\tau\tau} \lesssim 0.3$) and so the hadronic and two-photon backgrounds are substantial. A small systematic rise in the multi-prong electron production below charm threshold can be seen in Fig. 5. These data were selected automatically and a small improvement in background rejection is possible by manually scanning a computer reconstruction of each event. This has been carried out for events in the range $3.50 < E_{CM} < 3.725$ GeV and the resultant R_e plot (Fig. 15) provides direct evidence for the existence of τ decays into three-or-more charged particles.

B. Branching Ratios

The majority of the τ decay rates can be calculated and so branching-ratio measurements test whether the standard weak current participates in τ decays. The muon decay rate determines $\Gamma(\tau^- \to e^- \bar{\nu}_e \nu_\tau)$ and $\Gamma(\tau^- \to \mu^- \bar{\nu}_\mu \nu_\tau)$ and the pion lifetime measures $\Gamma(\tau^- \to \pi^- \nu_\tau)$. The experimental measurements of $e^+e^- \to n\pi$ (n-even) at $\sqrt{s} < m_\tau$ are related to $\tau^- \to (n\pi)^- \nu_\tau$ (n-even) via CVC. The τ axial-vector decay rates involving odd numbers of pions are less well-known

but are estimated using Weinbergs sum rules.[16] The small decay rates involving strange particles are related to the multi-pion calculations via $\tan^2\theta_c$. Recent theoretical calculations,[17] are summarized in Table 2 for τ decays into one-charged-particle plus neutrals.

Table 2

τ One-Prong Relative Rates and Branching Ratios

$\tau^- \to \nu_\tau$ +	Relative Rate	Branching Ratio (normalized to $b_e = 0.160$)
$e^- \bar{\nu}_e$	1.00	0.160
$\mu^- \bar{\nu}_\mu$	0.97	0.155
π^-	0.59	0.094
$\pi^-\pi^o$	1.24	0.198
$\pi^- + \geq 2\pi^o$	0.27	0.043
K^-	0.03	0.005
$Kn\pi$	0.05	0.008
		0.66 (Total)

The leptonic branching ratios are the most precisely measured among τ decays. The branching ratio for $\tau^- \to e^- \bar{\nu}_e \nu_\tau$ (denoted b_e) is provided by the fit in Fig. 12a) which yields $2\, b_e b_{x,0\gamma} = 0.105 \pm 0.007$, where $b_{x,0\gamma}$ is the branching ratio for $\tau^- \to \nu_\tau$ + 1 charged particle ($\neq e$) + no detected photons. The value of $b_{x,0\gamma}$ requires theoretical input of the rates, relative to $\tau^- \to e^- \bar{\nu}_e \nu_\tau$, of the decay modes $\mu^- \bar{\nu}_\mu \nu_\tau$, $\pi^- \nu_\tau$ and $\pi^-\pi^o \nu_\tau$. Approximately one-third of the $\pi^-\pi^o$ decays contribute, corresponding to events where both photons escape detection. After accounting for small contributions from decays involving larger pion multiplicities we determine,

$$b_e = 0.160 \pm 0.013$$

The error, which is largely systematic, is rather small since this determination of the cross section is proportional to b_e^2.

The validity of this approach depends on the existence of the three specified decay modes with the correct relative rates. Each are considered to be on solid theoretical ground and consequently the apparent absence of $\tau^- \to \pi^- \nu_\tau$, reported[18] by DASP at the Hamburg Conference last year, led to a variety of new descriptions of the nature of the τ.

The measurement of the branching ratio for $\tau^- \to \pi^- \nu_\tau$ (denoted b_π) clearly became an important goal. However, experimentally it is difficult since not only is the branching ratio low but also muon backgrounds must be removed, and this substantially reduces the data sample.

The first step in our analysis involves the isolation of a clean sample of τ decays by selecting two-prong eX events according to the previous criteria. In addition, the X particle is required to aim within a restricted sensitive area of the muon detector and have sufficient momentum to penetrate (typically 0.7 GeV/c).

There are 54 events which survive the selection criteria, corresponding to a sample of 27,800 $\tau^+\tau^-$ decays in the energy range, $3.57 < E_{CM} < 7.4$ GeV. We summarize these data in Table 3 according to particle composition.

Table 3

Predicted and Observed Event Category of the eX events

Event Category	Predicted Events $\tau^+ \to \nu_\tau\ e^+ \nu_e$, $\tau^- \to \nu_\tau\ Y$				Observed Events (ee background previously subtracted)
	$Y=\mu^- \bar{\nu}_\mu$	$Y=\pi^-$	$Y=\rho^-, A_1^-, K^-$ etc.	Total	
$e\mu$	14.7	2.0	1.0	17.7	23 (0)
$e\mu+\geq 1\gamma$	0	0	1.0	1.0	2 (0)
$e\pi$	0.8	12.4	6.1	19.3	17.4(0.6)
$e\pi+\geq 1\gamma$	0	0	6.4	6.4	9.5(1.5)

The predicted numbers of events in Table 3 are based on the previous branching ratios (Table 2) and include small additional contributions from multi-prong τ decays (0.2 events) and charm semi-leptonic decays (0.3 events). The experimental data show good agreement with the theoretical expectations. In particular, if the $\pi\nu_\tau$ (and $K\nu_\tau$) decay modes are absent, the predicted signal of $e\pi+0\gamma$ events would be 6.9-0.7 ($K\nu_\tau$) = 6.2 in contrast to 17.4 events observed. The probability for this to be a fluctuation is $<< 10^{-3}$.

We conclude that the decay $\tau^- \to \pi^- \nu_\tau$ exists and measure its branching ratio, $b_\pi = 0.094\ (17.4-6.9)/12.4$ i.e.

$$b_\pi = 0.080 \pm 0.032 \pm 0.013$$

Similarly we measure, $b_\mu = 0.155\ (23-3.0)/14.7$ i.e.

$$b_\mu = 0.21 \pm 0.05 \pm 0.03$$

The observed μ and π momentum spectra (Figs 16a) and 16b) are consistent with those expected from τ decays and in particular we observe that the pions do not cluster at the low momentum cut, which would suggest large

μ or multipion contamination. Both these branching ratio measurements are consistent with the hypothesis that the τ couples to the standard weak current.

We will now consider b_{mp}, the branching ratio for $\tau^- \to \nu_\tau + \geq$ (3 charged particles)$^-$. This has been determined in three independent ways. The fit to the data of Fig. 12b) determines $2b_e\,(1-b_e-b_{mp}) = 0.168 \pm 0.008$ which yields (for $b_e = 0.160$),

$$b_{mp} = 0.32 \pm 0.05$$

The direct observation of multi-prong τ decays (Fig. 15) gives a quantitatively somewhat weaker result, $2b_e\, b_{mp} = 0.092 \pm 0.021$ or,

$$b_{mp} = 0.29 \pm 0.07$$

Finally, we may plot (Fig. 17) the ratio of observed multi-prong to two-prong electron events, $R' = N(e^\pm + \geq 2\text{-prongs})/N(e^\pm + 1\text{ prong})$ above a minimum electron momentum. This ratio falls as the cutoff momentum is raised reflecting the relatively soft electron spectrum resulting from charm decays. Above ∿1.1 GeV/c momentum the ratio has the constant value of 1.9 ± 0.2 and indicates a common source for the electrons in both the multiprong and twoprong data. The value of b_{mp} is given by $(b_{mp}\,\varepsilon_{mp})/(b_x\,\varepsilon_x) = 1.9 \pm 0.2$, where $\varepsilon_{mp,x}$ are the appropriate detection efficiencies and $b_x = 1-b_e-b_{mp}$. (Note that the electron detection efficiency cancels and the dependency on b_e is fairly weak.) The result is,

$$b_{mp} = 0.34 \pm 0.05$$

All three determinations agree within errors and are averaged to give the final result,

$$b_{mp} = 0.32 \pm 0.04.$$

At present we have not made detailed studies of the composition of the τ multiprong decays. However it is clear from the uncorrected prong distribution of multiprong electron data taken below charm threshold (Fig. 18a) that the majority involve only three charged particles. The total pion

multiplicity will require a measurement of π^o production as indicated by the observed photon distribution (Fig. 18b)). (In order to decrease backgrounds these data have the additional requirement that the electron momenta exceed one third of the beam energy).

C. Characteristics of the τ-ν_τ-W Vertex

So far we have seen that the data support the hypothesis that the τ is a spin 1/2 lepton which, according to branching ratio measurements, couples to the conventional intermediate vector boson. It is therefore natural to assume that the e-ν_e vertex in the decay $\tau \to \nu_\tau\, e\nu_e$ is pure V-A and to use the electron energy spectrum to measure the V, A structure of the τ-ν_τ vertex. The most general coupling is a linear combination of V and A amplitudes but, for a massless ν_τ, the anticipated couplings are pure V-A or V+A which correspond, respectively, to a left-handed ν_τ and a right-handed ν_τ.

The shape of the electron spectrum in the τ rest frame is determined by the one-parameter Michel formula:

$$d\Gamma(x) = G_1 \left[3(1-x) + 2\rho\left(\frac{4}{3}x-1\right) + r(x)\right] x^2\, dx$$

where $G_1 = G^2\, m_\tau^5/48\pi^3$

and $x = 2\, p_e/m_\tau$ is the scaled energy of the electron

$(0 < x < 1)$. A V-A coupling is characterized by a Michel parameter, $\rho = 0.75$ and results in the spectral shape, $d\Gamma(x) \propto (3-2x)x^2dx$. In the case of V+A, $\rho=0$ and the electron spectrum becomes $d\Gamma(x) \propto (1-x)\, x^2\, dx$. We see that a V-A coupling results in the most probable electron energy at x=1 (as familiar in μ decay) whereas a V+A spectrum peaks at x=2/3 and is indeed zero at x=1. (Physically, the reason for this zero is that a

right-handed ν_τ leads to a total angular momentum 3/2 at x=1.) Other combinations of V and A are characterised by intermediate values of ρ e.g. pure V or pure A, corresponding to equal left-right amplitudes, implies $\rho = 3/8$.

The function r(x) accounts for radiative corrections to the standard spectral formula. Ali and Aydin[19] point out that the corrections can be approximately accommodated into the bare formula by using an effective Michel parameter, ρ_{eff}. They determine a substantial softening of the electron energies e.g. in the range $0.2 \leq x \leq 0.95$, $\rho_{eff} = 0.66$ for V-A and $\rho_{eff} = -0.18$ for V+A.

The experimental electron spectrum (Fig. 19a)) has been obtained from a sample of 621 eX + $\geq 0\gamma$ events in the range $3.57 \leq E_{CM} \leq 7.4$ GeV (ψ'' excluded). The spectrum observed below charm threshold (Fig. 19b)) is statistically weaker but benefits from a reduced Lorentz smearing and consequent higher sensitivity. The events were selected according to the criteria described earlier with a further requirement of at least one associated spark on the outer WSC for each track in order to provide a momentum measurement. In addition events were rejected if $|\vec{P}_e|+|\vec{P}_x|+|\vec{P}_e + \vec{P}_x| > 0.85\ E_{CM}$ in order to remove residual $e^+e^-\gamma$ and grossly mis-measured events. (The latter occur if a spark in the outer WSC is incorrectly assigned to a track in the MWPC.)

We summarize in Table 4 the fit results[20] for pure V-A and V+A and for the ρ parameter giving the minimum χ^2. At this stage we have not explicitly included radiative corrections in the Monte-Carlo-generated spectra and so it is appropriate to compare the observed Michel parameter approximately with $\rho_{eff} \sim 0.64$(V-A) and -0.17 (V+A).

Table 4

Summary of the Fits to the Data of Fig. 19

Hypothesis	a) All Data			b) Below Charm Threshold		
	ρ	χ^2	# dof	ρ	χ^2	# dof
V-A	0.75	13.8	17	0.75	8.1	7
V+A	0.0	57.9	17	0.0	21.7	7
Free Fit	$0.86\pm0.12\ \pm0.15$	13.0	16	$0.99\pm0.26\ \pm0.17$	7.2	6

We conclude that there is good agreement with a V-A coupling whereas V+A is completely excluded and pure V or pure A are disfavoured.

It is interesting to note[21] that these data are the first to exclude the Pati-Salam integer-charged quark[22] interpretation of the anomalous two-prong lepton events. In this model the events arise by decay of a pair of unconfined, pointlike, spin 1/2 quarks through intermediate real vector gluons in the process,

$$e^+e^- \to q^+ q^-$$
$$\hookrightarrow \nu_e V^- \to \nu_e e^- \bar{\nu}_e$$
$$\hookrightarrow \bar{\nu}_e V^+ \to \bar{\nu}_e \begin{cases} \mu^+ \nu_\mu \\ \text{hadrons} \end{cases}$$

The model is excluded on two counts:

i) Below q threshold there should remain a signal of eX events, with an electron spectrum characteristic of two-body decay, arising from direct pair production of vector gluons,

$$e^+e^- \to V^+V^- \to e^+ \nu_e \mu^- \bar{\nu}_\mu$$

This contradicts the observations made at E_{CM}= 3.50 and 3.52 GeV (Fig.13).

ii) The observed electron spectra (Fig. 19a) particularly below 0.5 GeV/c, are in complete disagreement with gluon decay for any value of its mass.[21]

The effect of a non-zero ν_τ mass is to soften the electron spectrum. Since the V+A hypothesis is ruled out for any value of m_{ν_τ} we set the ρ parameter at 0.64 (V-A) and 0.86 (minimum χ^2) for this study. From the measured χ^2 variations with non-zero ν_τ masses[23] we determine,

$$m_{\nu_\tau} < 0.25 \text{ GeV}/c^2 \text{ (95\% CL)}$$

To summarize, it appears that the τ^- couples to a neutral object which is consistent with being massless and purely left-handed. However before simply introducing a new neutrino it is important to investigate whether the 'ν_τ' is actually one of the old neutrinos. Experimentally, the assignment $\nu_\tau = \nu_\mu$ has been excluded by neutrino experiments. Unfortunately, since ν_e beams are poor, they have not provided a test of the electron neutrino assignment. The latter possibility is unlikely since the branching ratio for $\tau^- \to e^-\gamma$ is small ($\leq$ 2.6% (90%CL) as measured by the SLAC-LBL group).

The exclusion of the old-neutrino assignment assumes a full-strength τ-ν_τ-W vertex. In a heavy-neutrino model with $m_{\nu_\tau} > m_\tau$ the τ would decay via a small mixing[24] between ν_e, ν_μ and ν_τ consistent with the experimental constaints from the neutrino experiments and μ-e-β universality.

An immediate consequence is that the τ lifetime (τ_o) is longer than that expected in the standard model, which predicts $\tau_o = \tau_\mu \, (m_\mu/m_\tau)^5 \, b_e$. For an electronic branching ratio of 0.16 this lifetime is $2.6 \, 10^{-13}$ sec which allows a flight path of about 0.1 mm at a beam energy of 3 GeV.

The experimental technique for measuring the lifetime is to determine the apparent origin of the individual prongs in the eX events. In order to increase the sensitivity, the following additional cuts are imposed. Only data above E_{CM}=6 GeV are considered and both tracks must be well-measured geometrically ($\geq$ 5 hits in the MWPC and at least one WSC spark in the ϕ and θ views) and have a minimum momentum of 300 MeV/c. Events are selected containing a high-energy prong (P > 1.35 GeV/c) and another track making a coplanarity angle between 60^{o} and 140^{o}. The high-energy prong presumably results from a forward decay of one τ and can therefore define the direction of the second τ. The apparent projected flight path of the second τ is determined by the distance of closest approach of the second prong from the beam centre. This technique has the merit of a known τ flight direction and, as a result of the angular cuts, the maximum sensitivity to a finite flight path.

The 35 events which survive these criteria do not display a systematic displacement away from the beam centre (Fig. 20b)). (The mean (μ) of the distribution is μ=0.025$\pm$0.19 mm). As a check of the procedure, the same analysis of multi-prong hadronic events (Fig. 20a)) also produced a centred distribution. (The latter check is really only meaningful in the absence of null result for the τ.) From Monte-Carlo studies we determine that a true $c\tau$ value of 1 mm leads to projected flight distance of 0.37 mm integrated over the E_{CM} range. We thereby determine the τ lifetime limit,

$$\tau_o < 2.8 \quad 10^{-12} \text{ sec (95\% CL)}$$

The heavy τ-neutrino model assumes that the ν_e-e and ν_μ-μ couplings are reduced by factors $(1-\varepsilon_e^{\,2})$ and $(1-\varepsilon_\mu^{\,2})$ due to a small coupling between the τ and the old neutrinos. The upper limit on the τ lifetime provides a

lower bound on the coupling strength to ν_e and ν_μ given by,

$$\tau_o = \frac{2.6\ 10^{-13}\ \text{sec}}{\varepsilon_e^{\,2} + \varepsilon_\mu^{\,2}}$$

$$\text{i.e.} \quad \varepsilon_e^{\,2} + \varepsilon_\mu^{\,2} > 0.09$$

The tight experimental limits on μ-e-β universality place upper bounds on the mixing amplitudes For example, the ratio of the coupling strengths (G′),

$$\frac{G'(K_{e3}) + G'(0^{14}\ \beta\ \text{decay})}{G'(\mu\ \text{decay})} = 1.003 \pm 0.004$$

This comparison removes the Cabibbo angle and indicates,

$$\varepsilon_\mu^{\,2} = 0.003 \pm 0.004$$

In addition,

$$\frac{\Gamma(\pi \to e\nu)}{\Gamma(\pi \to \mu\nu)} = \text{theory} \times (1.03 \pm 0.02)$$

$$\text{i.e.} \quad \varepsilon_\mu^{\,2} - \varepsilon_e^{\,2} = 0.03 \pm 0.02$$

The combination of these two results measures,

$$\varepsilon_\mu^{\,2} = 0.003 \pm 0.004 \text{ and } \varepsilon_e^{\,2} = -0.027 \pm 0.02$$

Therefore the total 'missing' coupling strength is

$$\varepsilon_e^{\,2} + \varepsilon_\mu^{\,2} = -0.024 \pm 0.02$$

We observe this is in contradiction with the lower bound provided by the τ lifetime measurement and hence the heavy τ neutrino possibility is excluded.

In conclusion, there is now a very solid case for the existence of the third charged lepton, τ, with all properties compatible with a coupling to its own massless neutrino and the standard intermediate vector boson. The τ is indeed ready to receive that ultimate accolade, 'ready for the text-books'.

Acknowledgements: I would like to thank my colleagues in the DELCO collaboration for their most enjoyable and informative company. In addition I acknowledge the invaluable services of the Experimental Facilities Division, SPEAR Operations Group and SLAC Computing Center.

References

1) The members of the DELCO collaboration are:
W. Bacino, T. Ferguson, L. Nodulman, W. Slater, H. K. Ticho, University of California, Los Angeles, California 90024, A. Diamant-Berger, G. J. Donaldson, M. Duro, A. Hall, G. M. Irwin, J. Kirkby, F. S. Merritt, S. G. Wojcicki, Stanford Linear Accelerator Center and Physics Department, Stanford University, Stanford, California 94305, R. Burns, P. Condon, P. Cowell, University of California, Irvine, California 92664, J. Kirz, State University of New York, Stony Brook, N.Y. 11794.

2) P. Rapidis et al., Phys. Rev. Lett. 39, 526 (1977).
W. Bacino et al., Phys. Rev. Lett. 40, 671 (1978).

3) Wherever two errors are quoted the first is statistical and the second is systematic.

4) G. Feldman. Raporteurs talk at the XIX International Conference on High Energy Physics, Tokyo, Japan (August 1978).

5) K. Gottfreid. Proceedings of the International Conference on Lepton and Photon Interactions at High Energies, (August 1977), edited by F. Gutbrod and published by DESY, Hamburg, Germany.

6) A. De Rujula and R. Jaffe, Proceedings of the Conference on Experimental Meson Spectroscopy, Northeastern University, Boston (April 1977).

7) C. Baltay, Proceedings of the International Conference on Neutrino Physics and Neutrino Astrophysics, Purdue University, (April 1978).

8) M. K. Gaillard, B. W. Lee and J. L. Rosner, Rev. Mod. Phys. 47, 277 (1975).

9) There has been extensive discussion of D semi-leptonic decays in the literature. The following is a partial list from which further references may be derived. J. Ellis, M.K. Gaillard and D.V. Nanopoulos, Nucl. Phys. B100, 313 (1975), A. Ali and T. C. Yang, Phys. Lett. 65B 275 (1976), I. Hinchliffe and C. M. Llewellyn-Smith, Nuc. Phys. B114 45 (1976), V. Barger, T. Gottschalk and R. Phillips, Phys. Rev. D16, 746 (1977), W. Wilson, Phys. Rev. D16, 742, F. Bletzacker, M. T. Nieh and A. Soni, Phys. Rev. D16, 732 (1977), D. Fabirov and B. Stech, Nucl. Phys. B133, 315 (1978).

10) G. Altorelli et al., Phys. Rev. Lett. 35, 635 (1975) and Nucl. Phys. B88, 285 (1975), Y. I. Wasak, Phys. Rev. Lett. 34, 1407 (1975), M. Einhorn et al., Phys. Rev. D12, 2013 (1975) and Phys. Rev. Lett. 35, 1407 (1975), M. Katuya et al., Nuovo Cimento Lett. 16, 357 (1976).

11) G. Feldman, Proceedings of the SLAC Summer Institute on Particle Physics SLAC-204 (1977).

12) R. L. Kingsley et al., Phys. Rev. D11, 1919 (1975).

13) R. Brandelik et al., Phys. Lett. 73B, 109 (1978).
W. Bacino et al., Phys. Rev. Lett. 41, 13 (1978).
W. Bartel et al., submitted to Phys. Lett.

14) Y. S. Tsai, SLAC-PUB-2105.

15) For clarity we shall only refer to one charged state of the τ.

16) Y.S. Tsai, Phys. Rev. D4, 2821 (1971),
H. B. Thacker and J. J. Sakurai, Phys. Lett. 36B, 103 (1971).

17) F. J. Gilman and D. H. Miller, Phys. Rev. D17, 1846 (1978),
N. Kawamoto and A. I. Sanda, DESY 78/14 (1978).

18) S. Yamada, Proceedings of the International Conference on Lepton and Photon Interactions at High Energies, (August 1977), edited by F. Gutbrod and published by DESY, Hamburg, Germany.

19) A. Ali and Z. Z. Aydin, Nuov. Cim. 43A, 270 (1978).

20) These measurements possess rather large systematic errors since, at present, the Monte-Carlo-generated spectra do not include radiative corrections or a detailed accounting of momentum measurement-error tails.

21) A. W. Ball and C. D. Froggatt, Glasgow University preprint 78-0953 (1978).

22) J. C. Pati and A. Salam, Proceedings of the 1976 Aachen Neutrino Conference, edited by H. Faissner et al.

23) We thank Y. S. Tsai for providing the analytic expressions for $m_{\nu_\tau} \neq 0$.

24) N. Cabibbo, XV Ettore Majorna School for Subnuclear Physics, Erice (1977), C. W. Kim, Johns Hopkins preprint HET-7804 (1978).

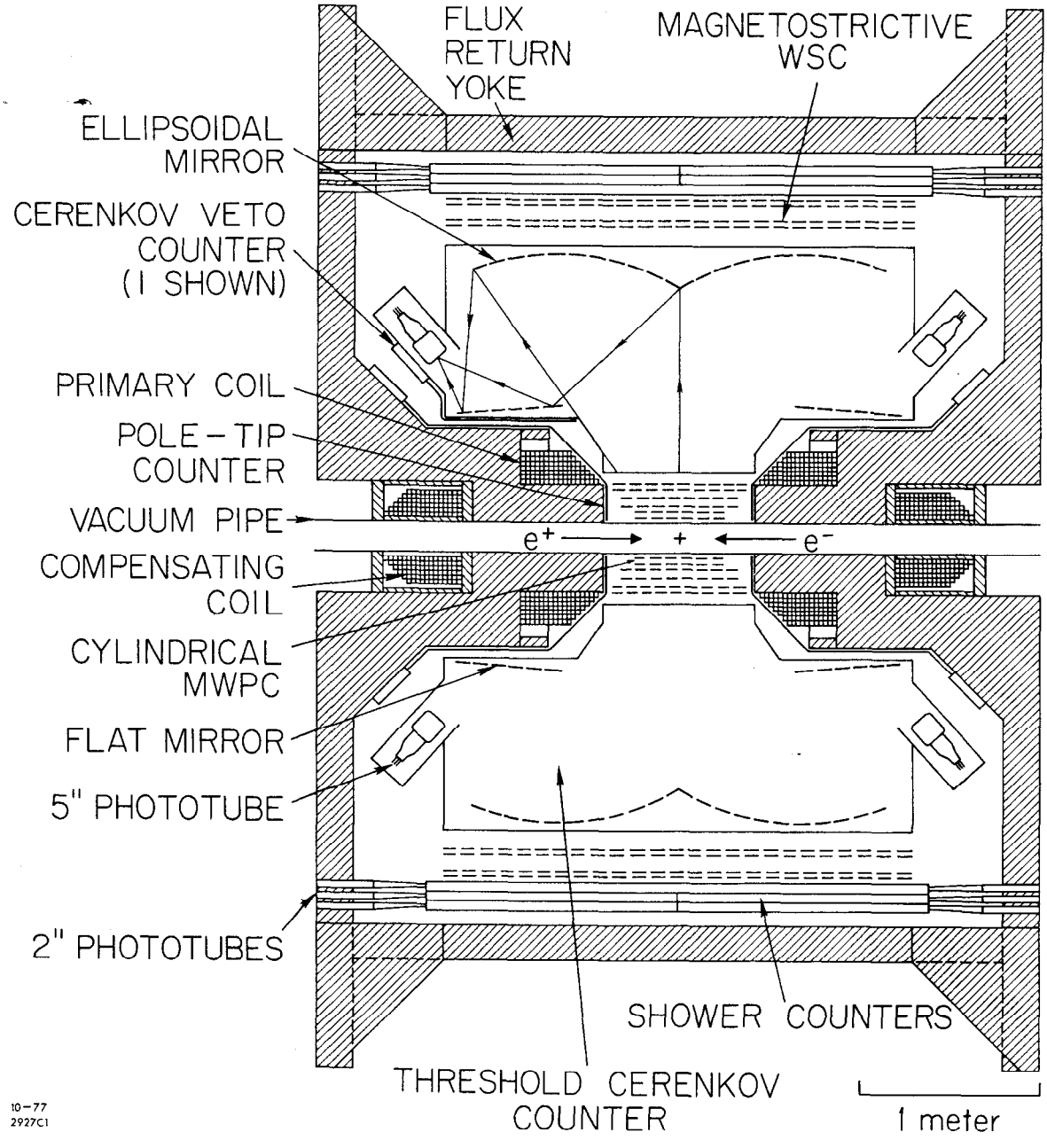

Fig. 1. a) Polar projections of the apparatus.

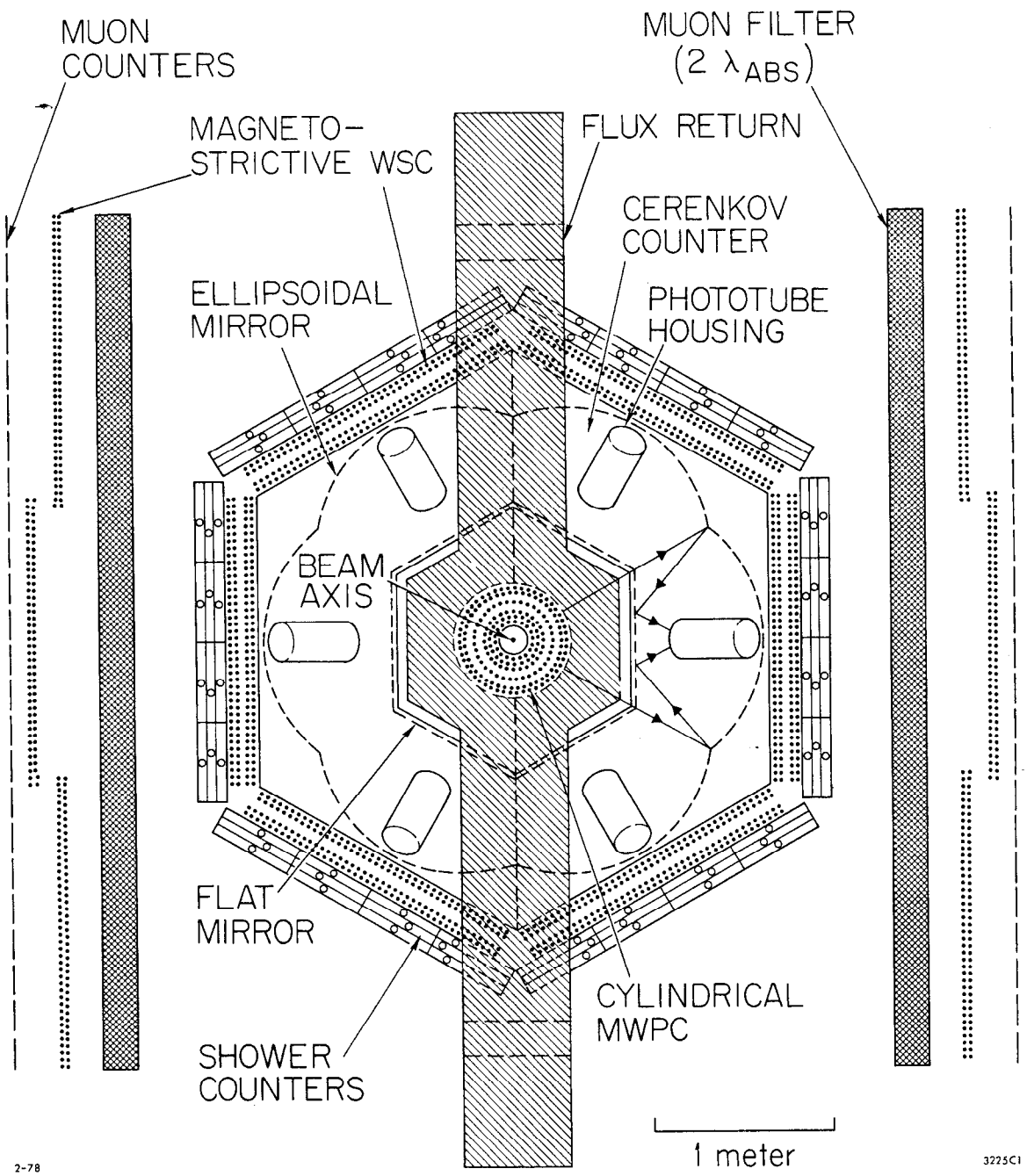

Fig. 1. b) Azimuthal projections of the apparatus.

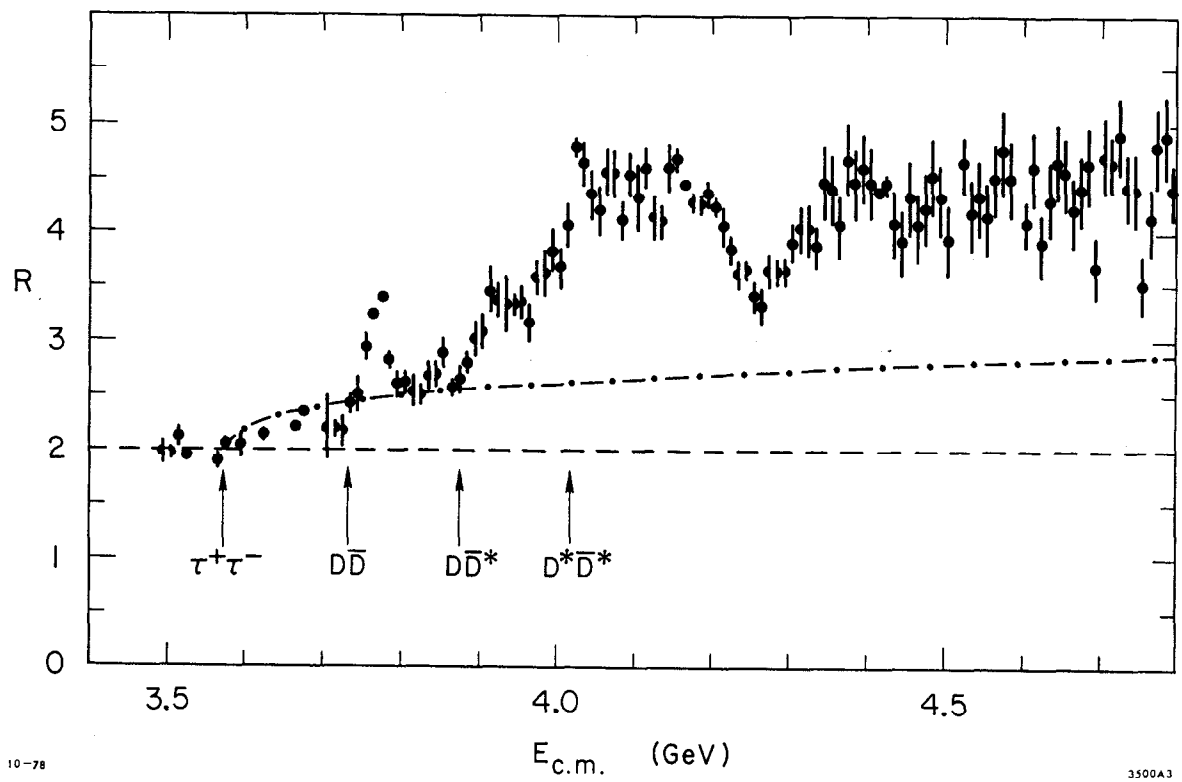

Fig. 2. The hadronic cross section, R in the range $3.50<E_{CM}<4.8$ GeV after removal of the ψ and ψ' radiative tails. The dashed line represents the contribution from old physics and the dot-dashed line is the τ contribution. Also indicated are the energy thresholds for τ and D production.

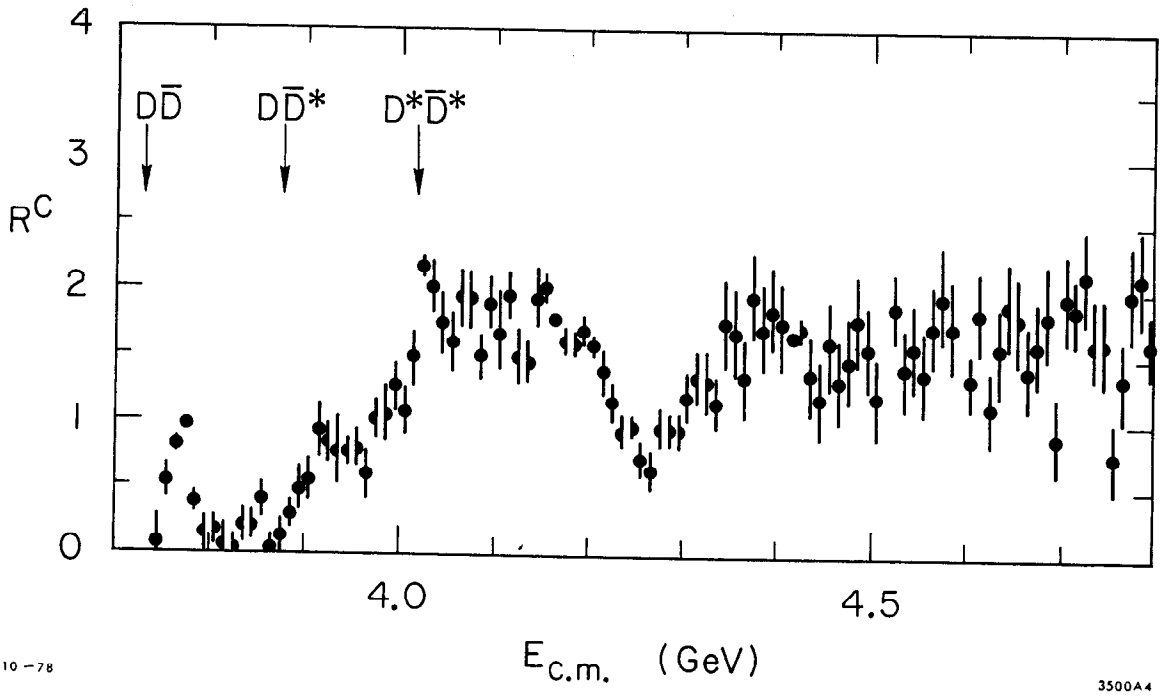

Fig. 3. The charm hadronic cross-section, R^c. The contributions from old physics, $\tau^+\tau^-$ pairs and the ψ and ψ' radiative tails have been removed.

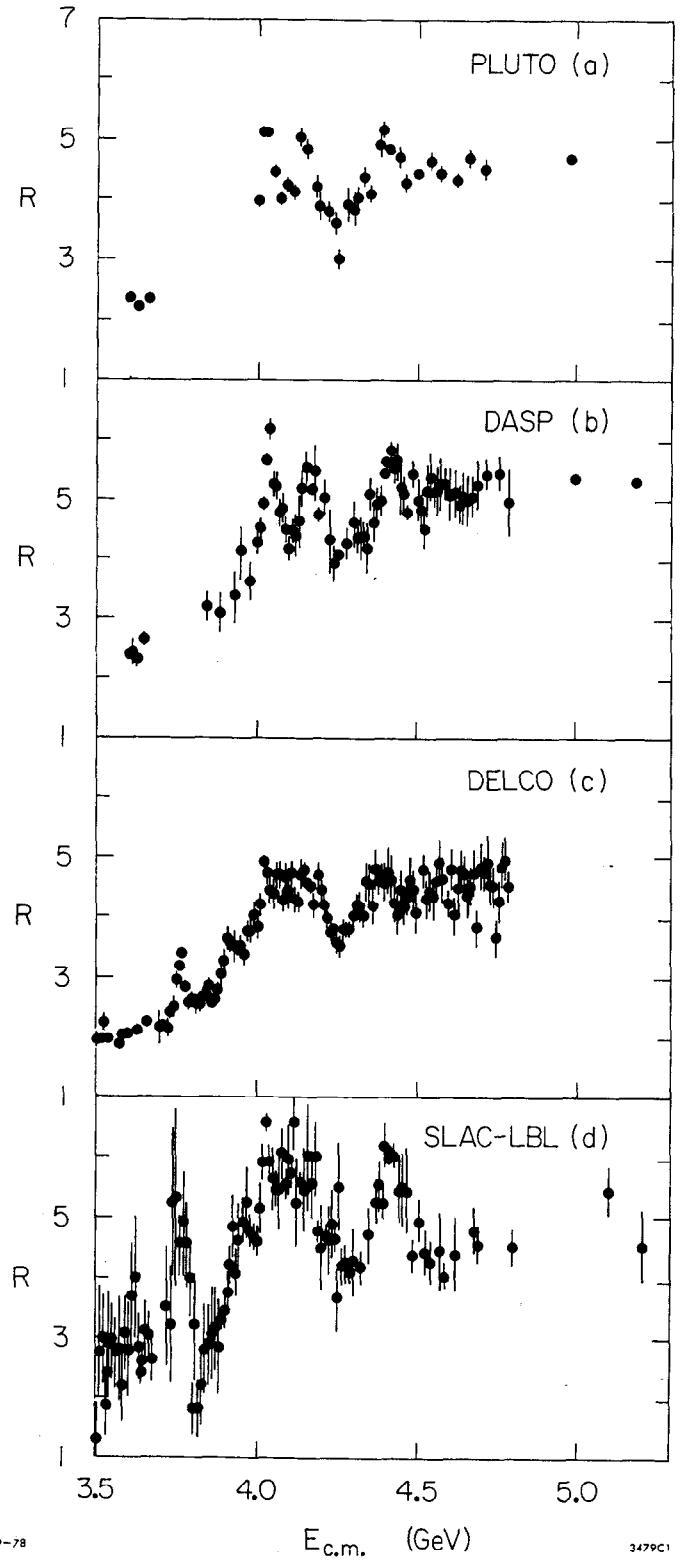

Fig. 4. A comparison of the hadronic cross sections from a) PLUTO b) DASP c) DELCO and d) SLAC-LBL. Complete radiative corrections have been applied to all data with the exception of those from DELCO (which displays the raw data after removal of the ψ and ψ' radiative tails).

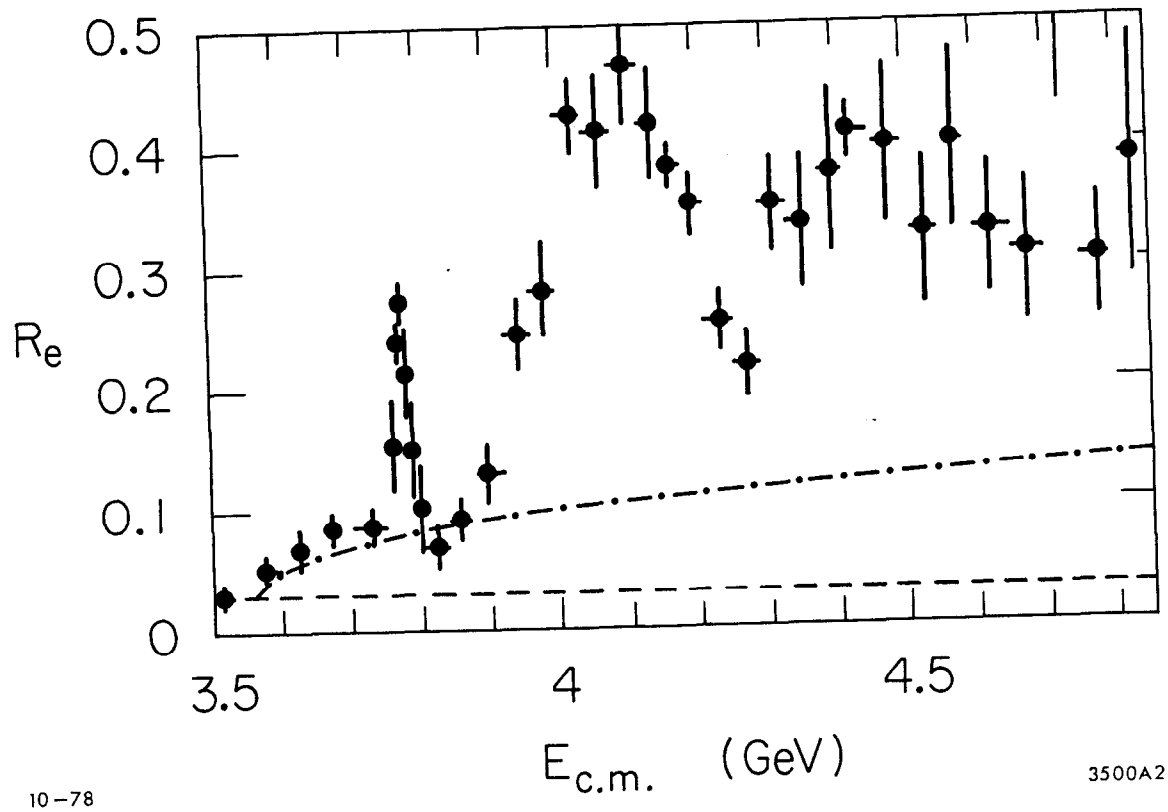

Fig. 5. The multi-prong electronic cross-section, R_e. The residual background is indicated by the dashed line and the dot-dashed line is the τ contribution.

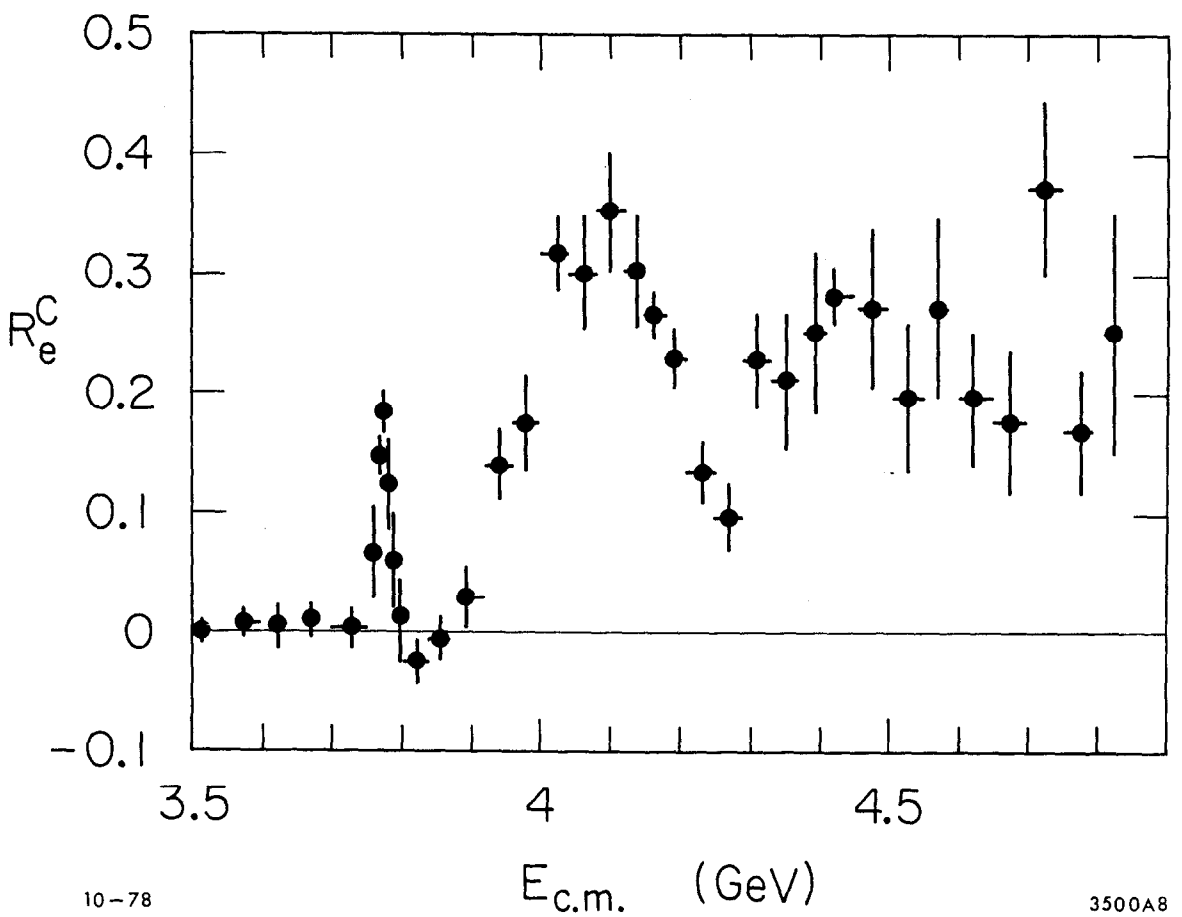

Fig. 6. The charm multi-prong electronic cross-section, R_e^c. The contributions from backgrounds and τ leptons have been removed.

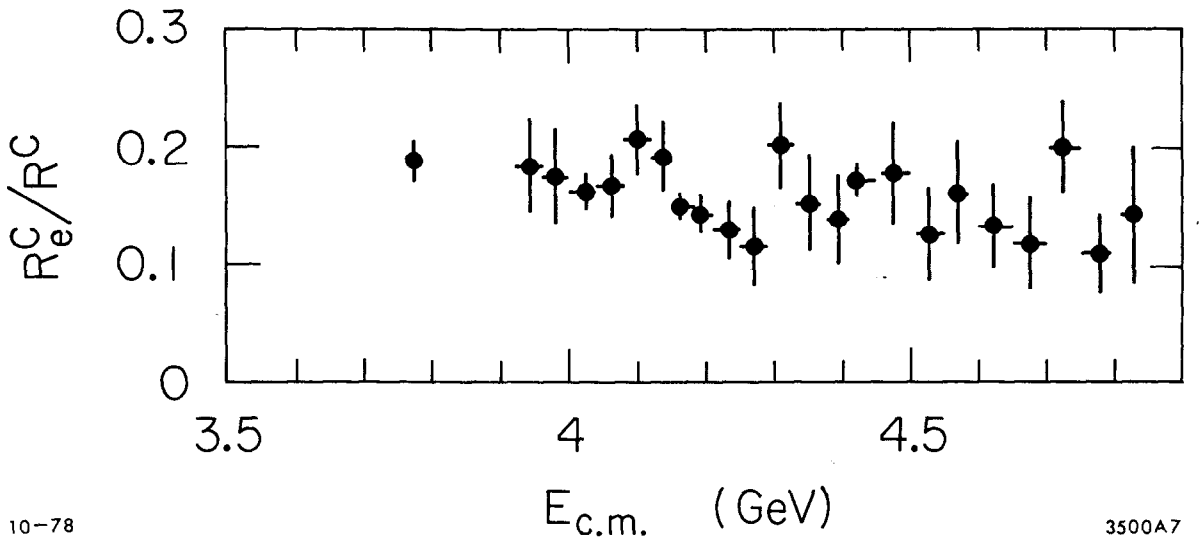

Fig. 7. The ratio R_e^c/R^c. The data are plotted where the ratio can be well determined (at E_{CM}=3.77 GeV and above E_{CM}=3.95 GeV). The error bars are statistical and do not reflect possible smooth energy-dependent systematic errors.

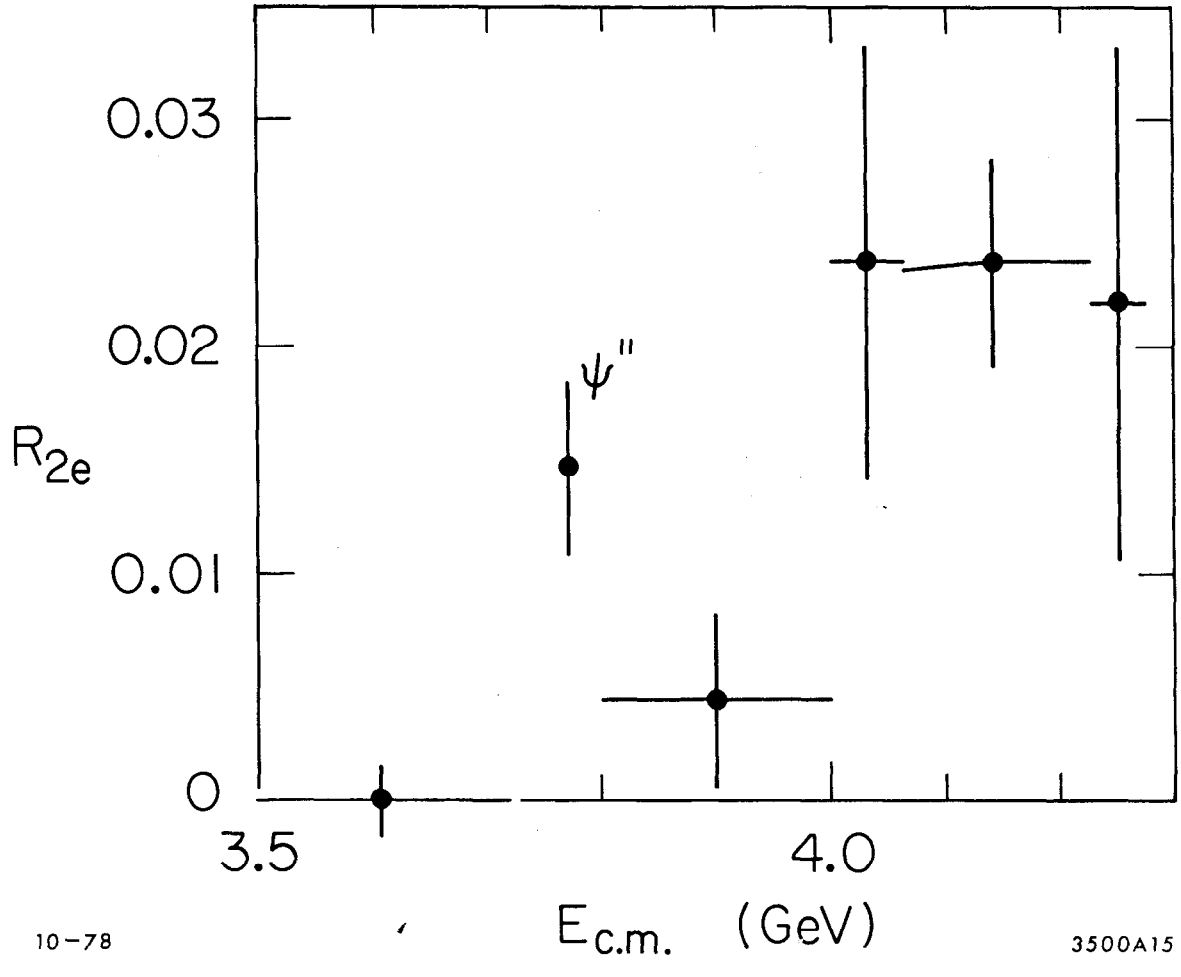

Fig. 8. The two-electron multi-prong cross-section, R_{2e}.

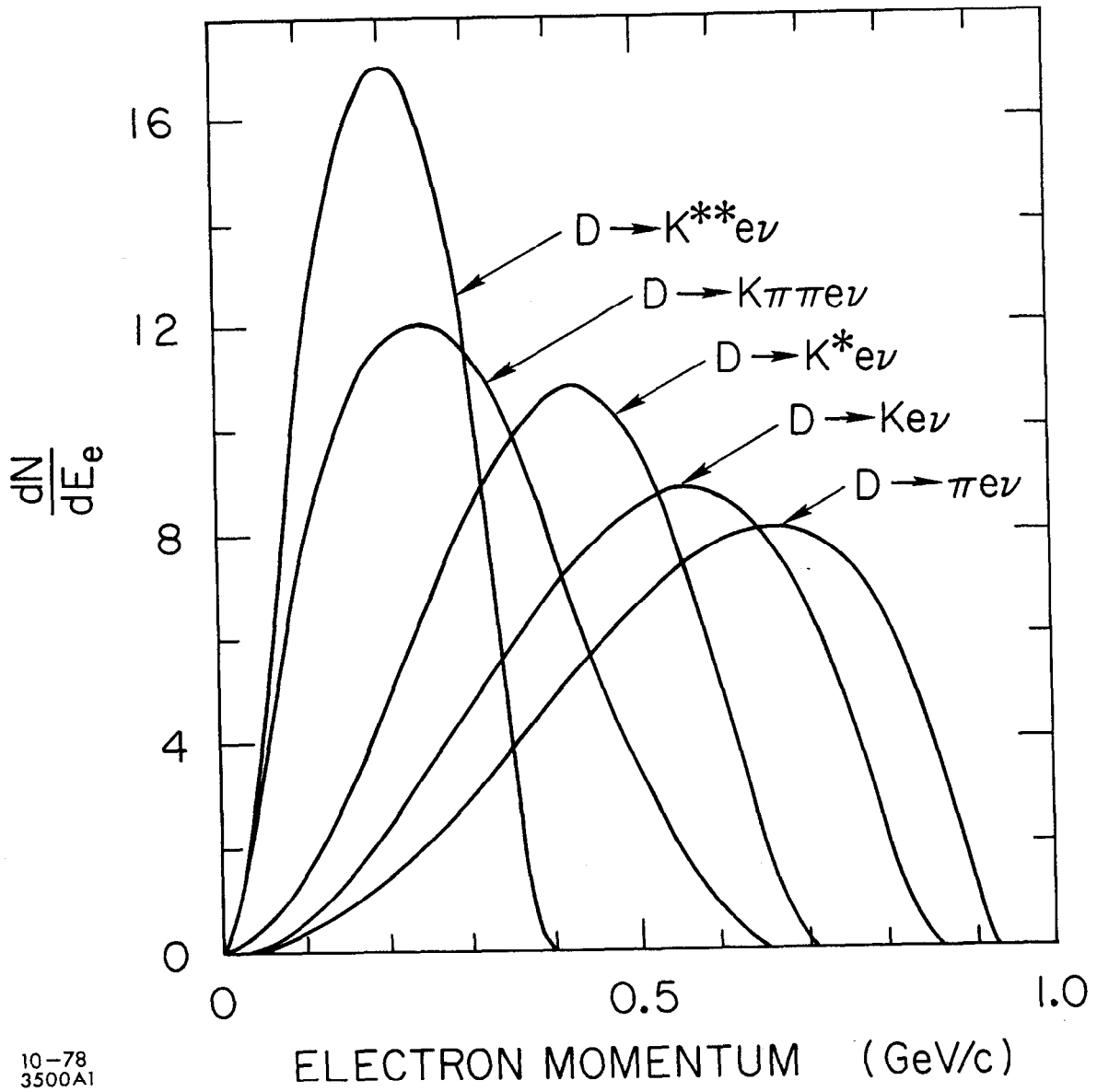

Fig. 9. The electron momentum spectra from several semi-leptonic decay modes of the D at rest.

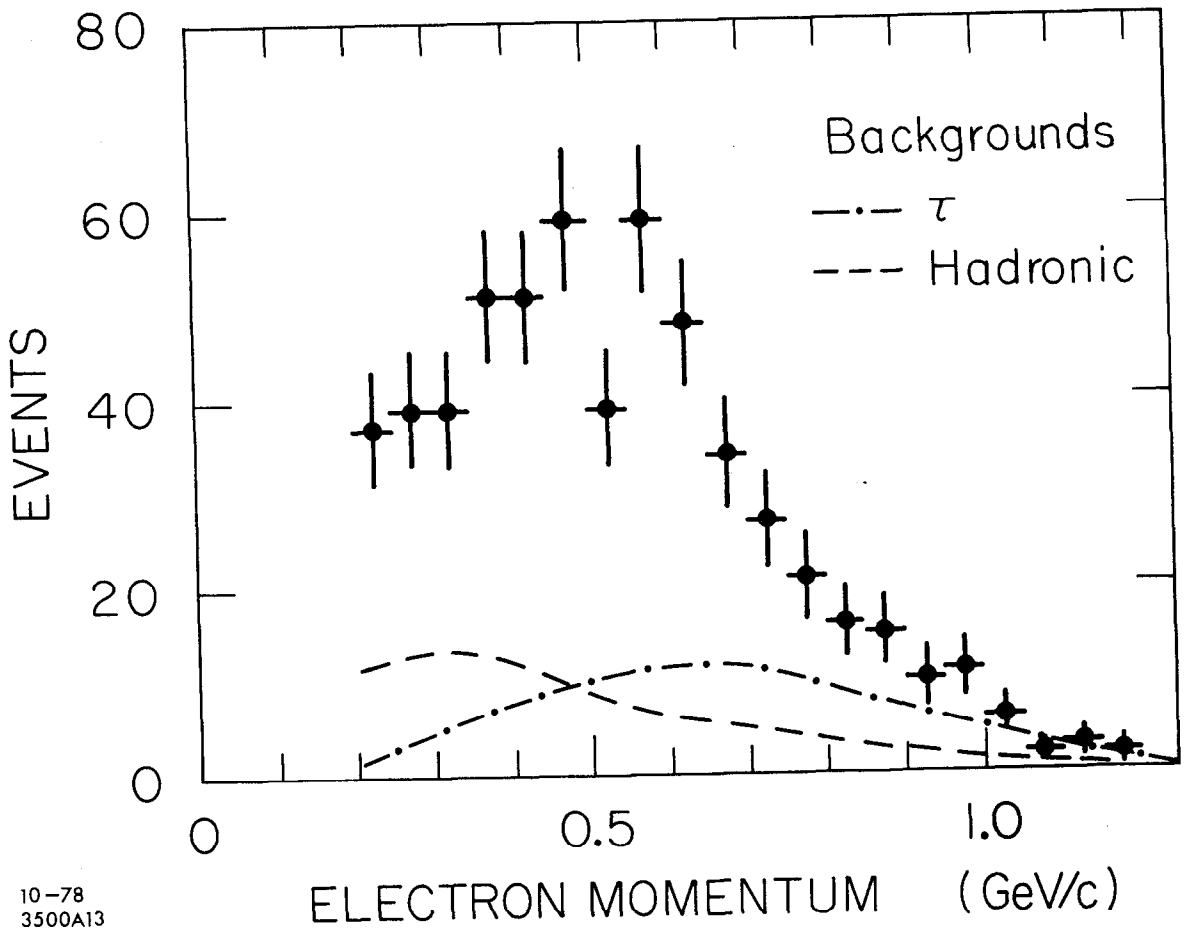

Fig. 10. The unsubtracted electron momentum spectrum obtained in the multiprong events at the ψ''. The backgrounds from the τ and other processes are indicated, respectively, by the dot-dashed and dashed lines.

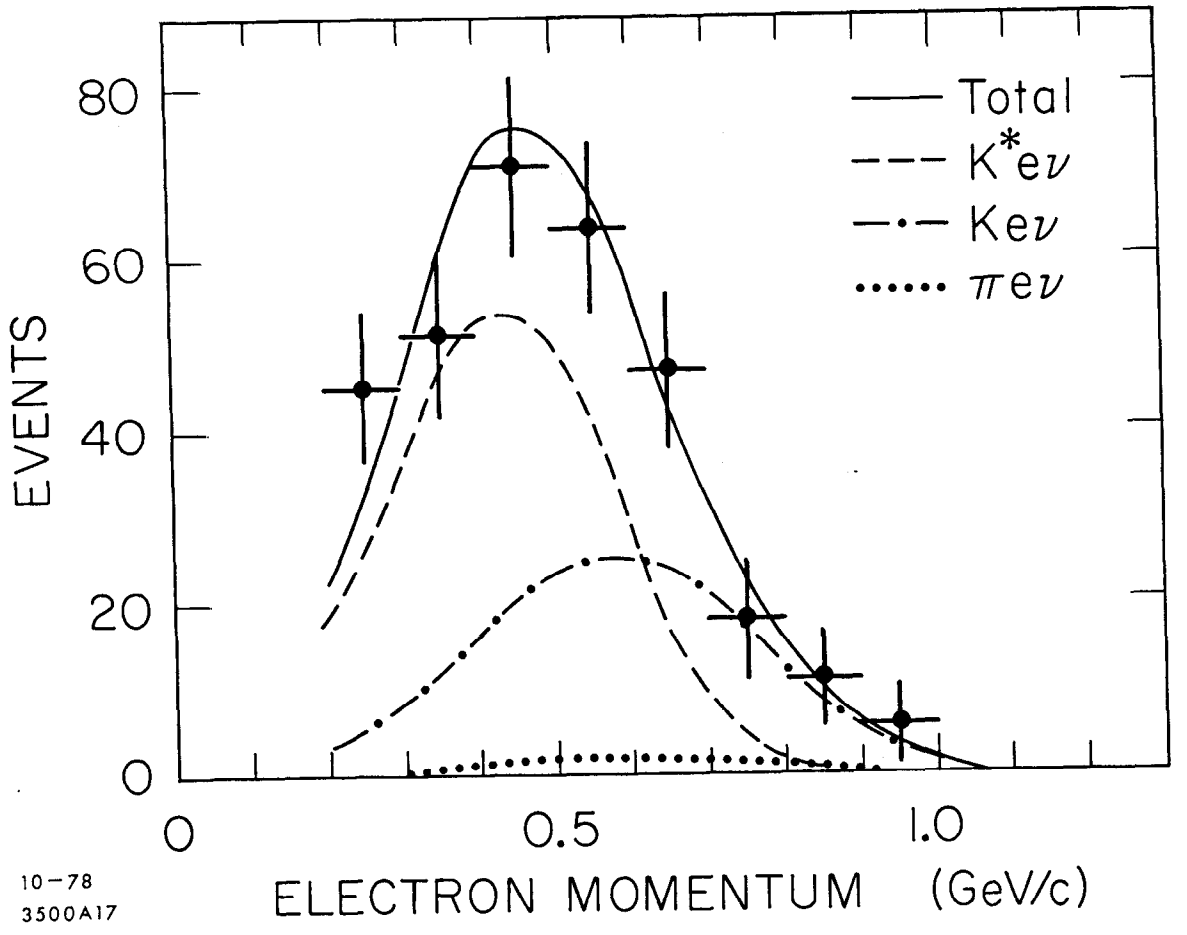

Fig. 11. The D electron momentum spectrum at the ψ''. The fits indicate the contributions from $K^{*}e\nu$ (dashed line), $Ke\nu$ (dot-dashed line) and $\pi e\nu$ (dotted line) to the total (solid line).

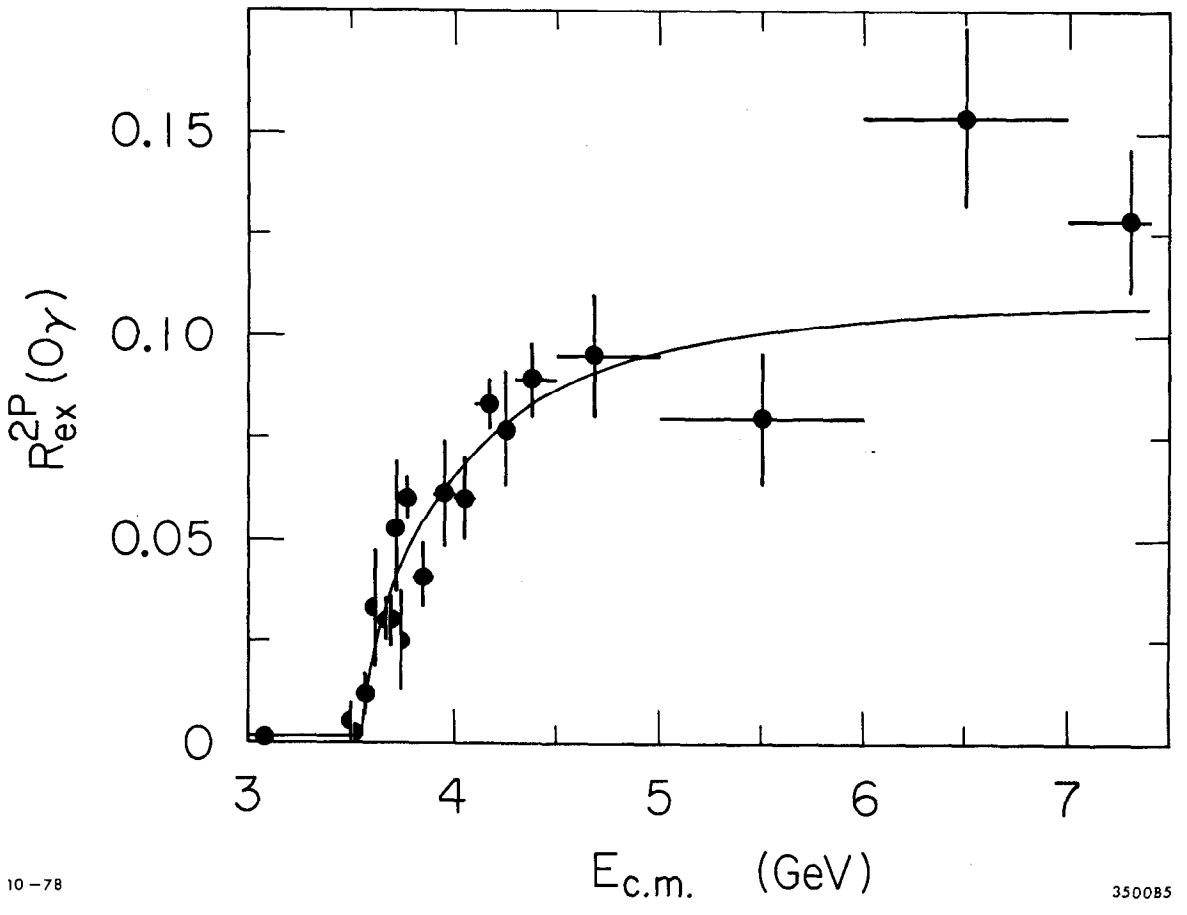

Fig. 12. a) The two-prong electronic cross section, R_{eX}^{2P} for eX events with no detected photons.

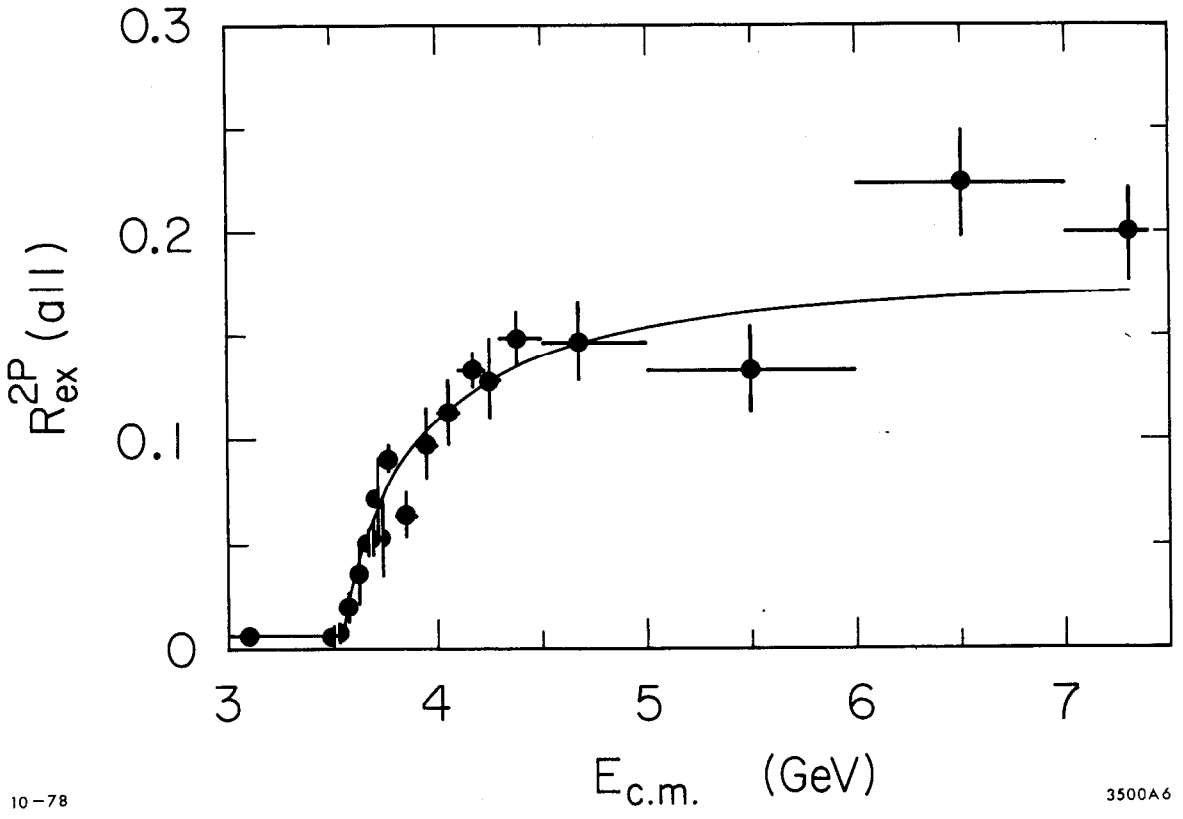

b) The two-prong electronic cross section, R_{ex}^{2P} for all eX events. The fitted curves indicates the cross sections expected from a spin 1/2 τ lepton after accounting for radiative corrections. Both fits have excluded the ψ'' point because of possible charm contamination.

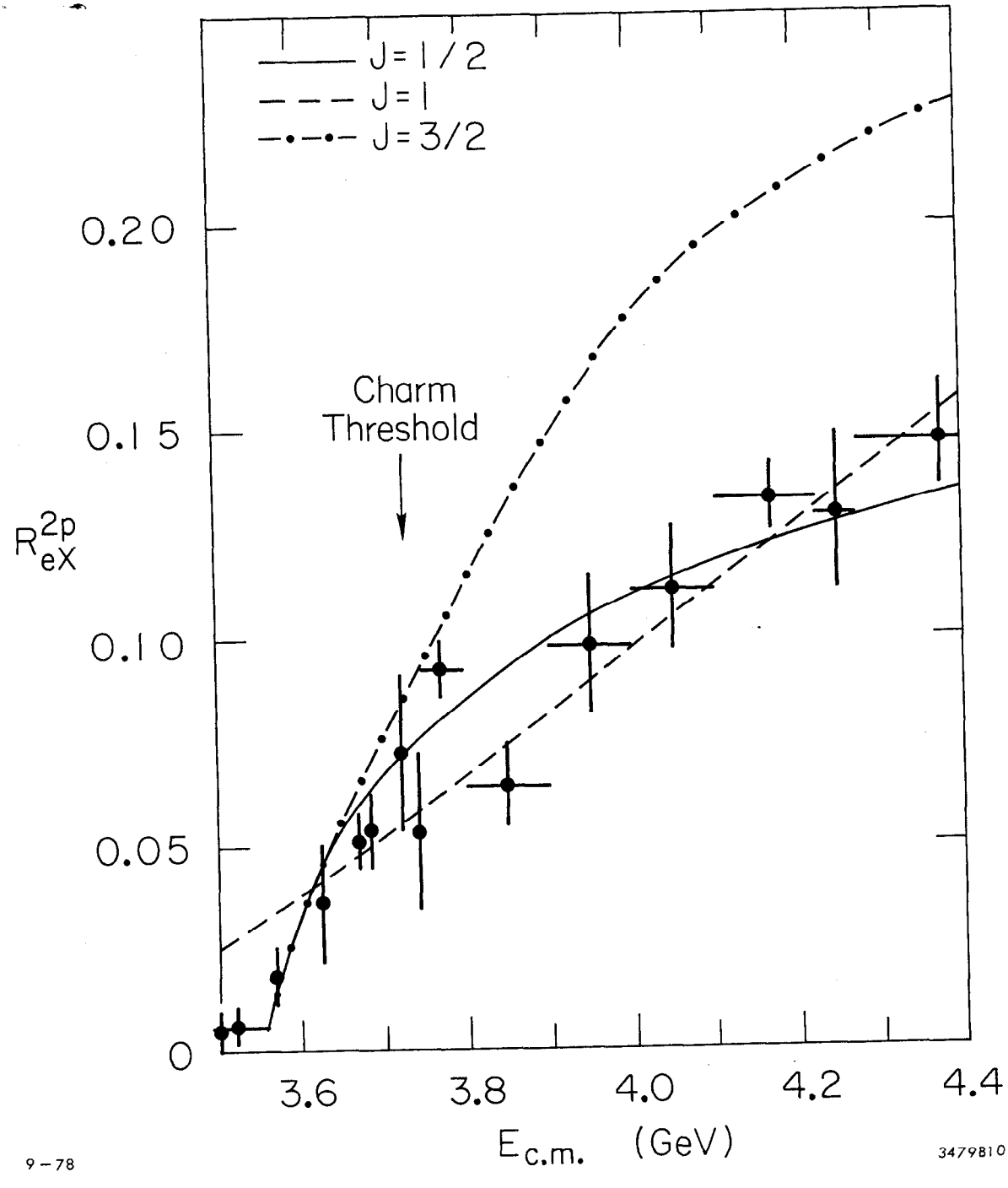

Fig. 13. R_{ex}^{2P} for all eX events with $3.50<E_{CM}<4.40$ GeV. The fitted curves indicate the (radiatively-corrected) threshold behaviour of a pair of particles with spin 1/2 (solid), 1 (dashed) and 3/2 (dot-dashed).

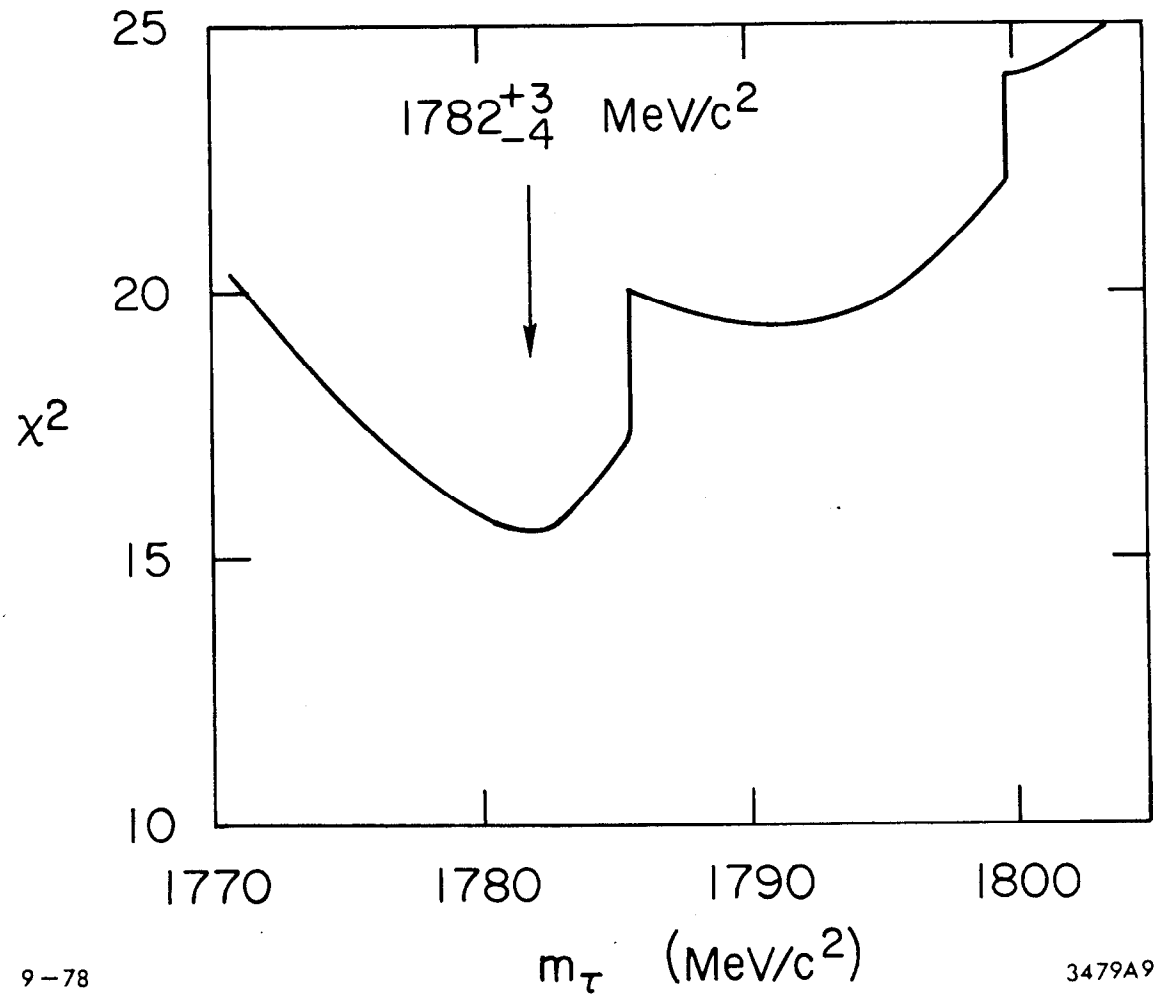

Fig. 14. Total χ^2 of the fit to the data of Fig. 12b) vs. τ mass ($E_{CM}/2$). The fit has 17 degrees-of-freedom.

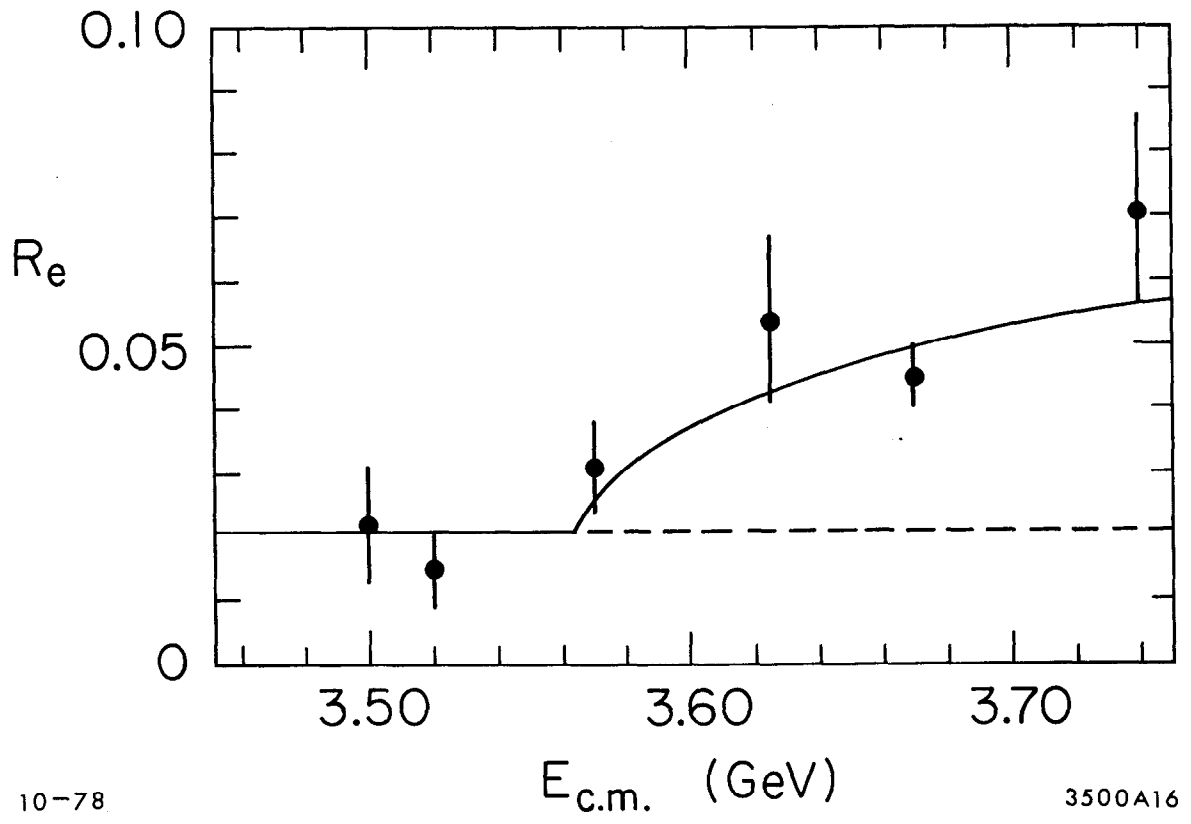

Fig. 15. R_e for the multi-prong electron data below charm threshold. The ψ' point is excluded. (The nearby point was taken below the ψ' at E_{CM}=3.67 GeV.) The fitted curve (χ^2/dof=4.1/4) corresponds to a spin 1/2 τ lepton, of mass 1782 MeV/c^2, superimposed on a constant background term.

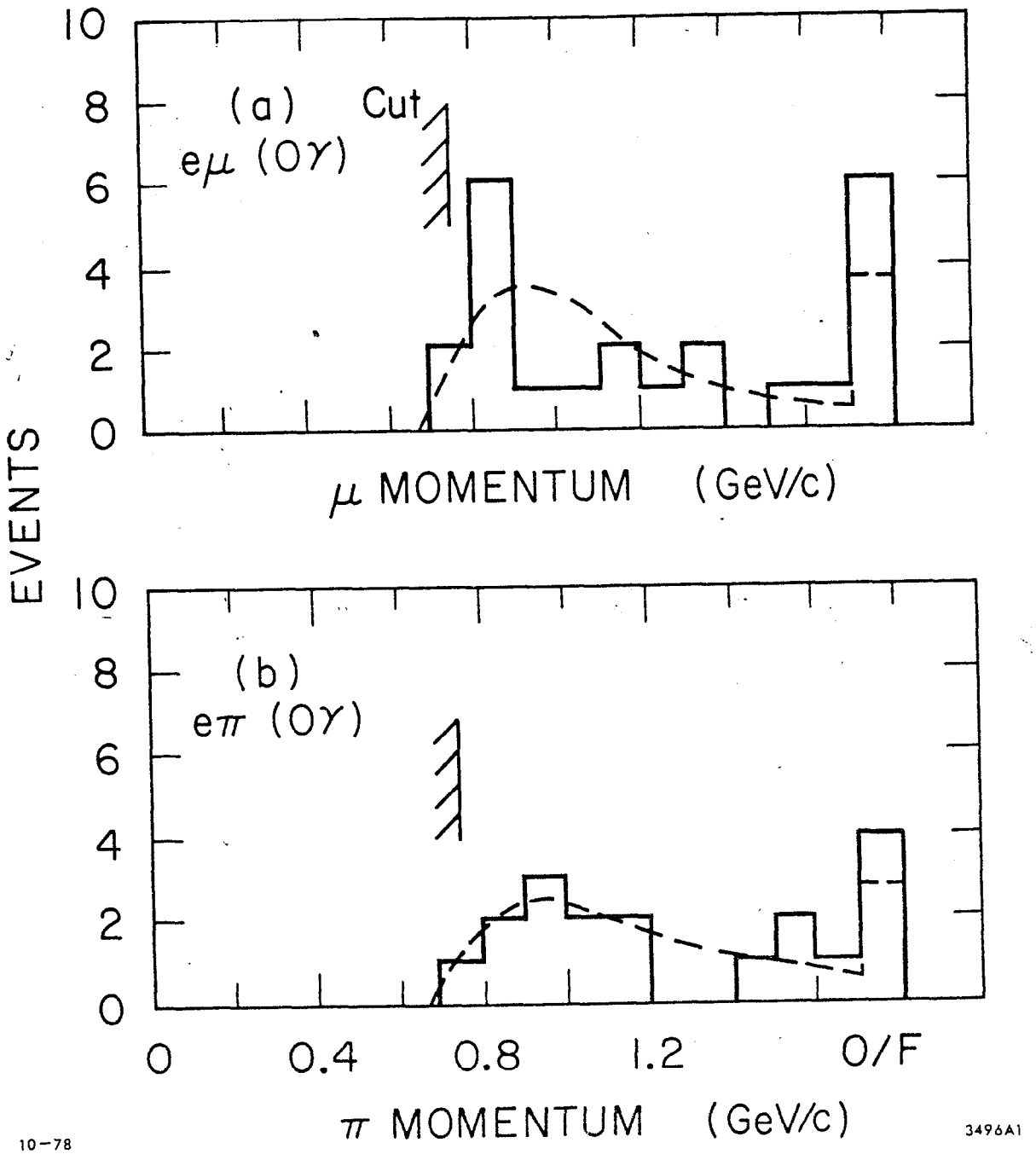

Fig. 16. a) Momentum spectrum of the μ in the eμ(0γ) events.

b) Momentum spectrum of the π in the eπ(0γ) events.

The dashed lines indicate the predicted shapes expected from τ decays. The cut indicated corresponds to the average amount of material a track must penetrate to be identified by the muon detector.

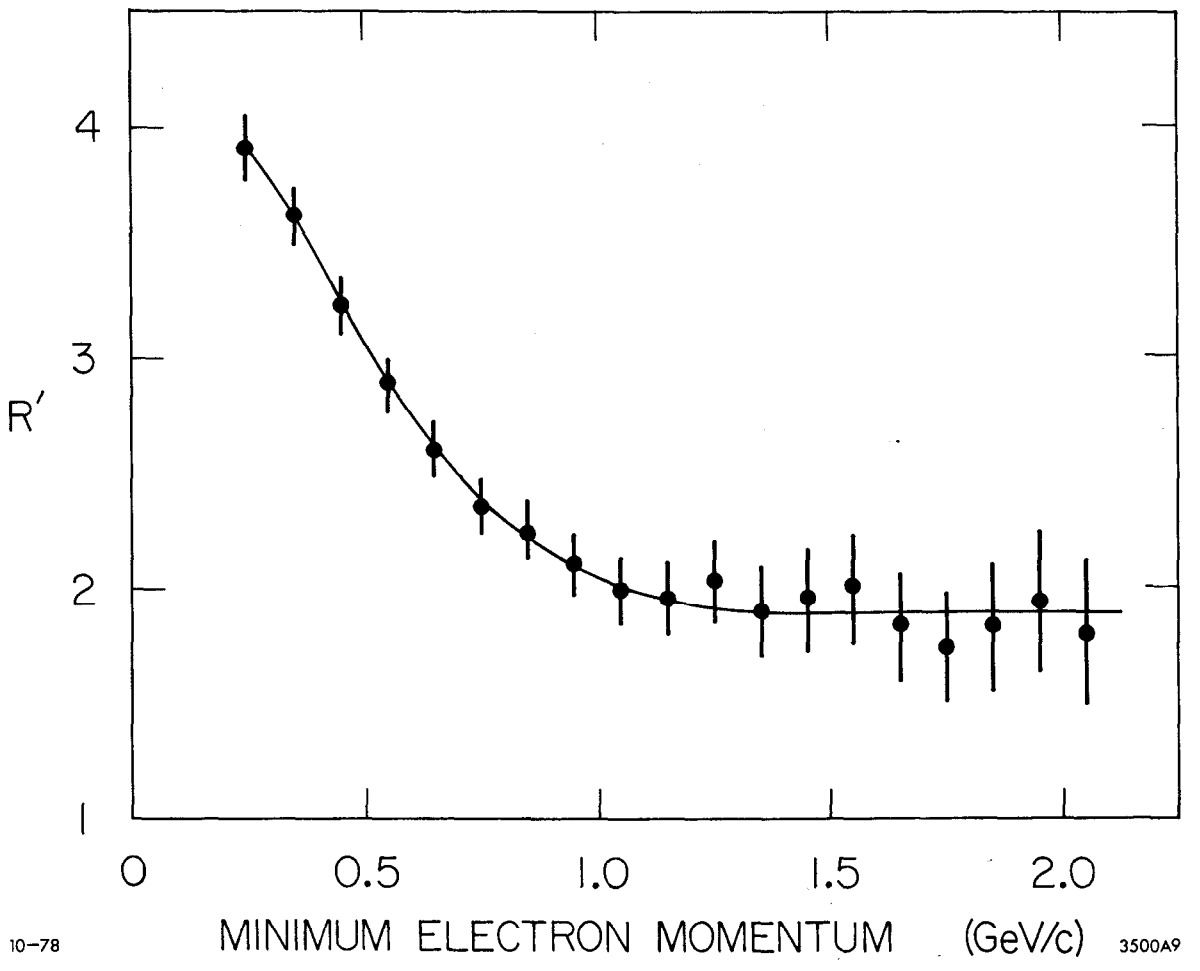

Fig. 17. The ratio, R′, of the observed multi-prong electron events to the observed two-prong electron events at electron momenta above the value indicated on the horizontal axis. The curve is hand-drawn.

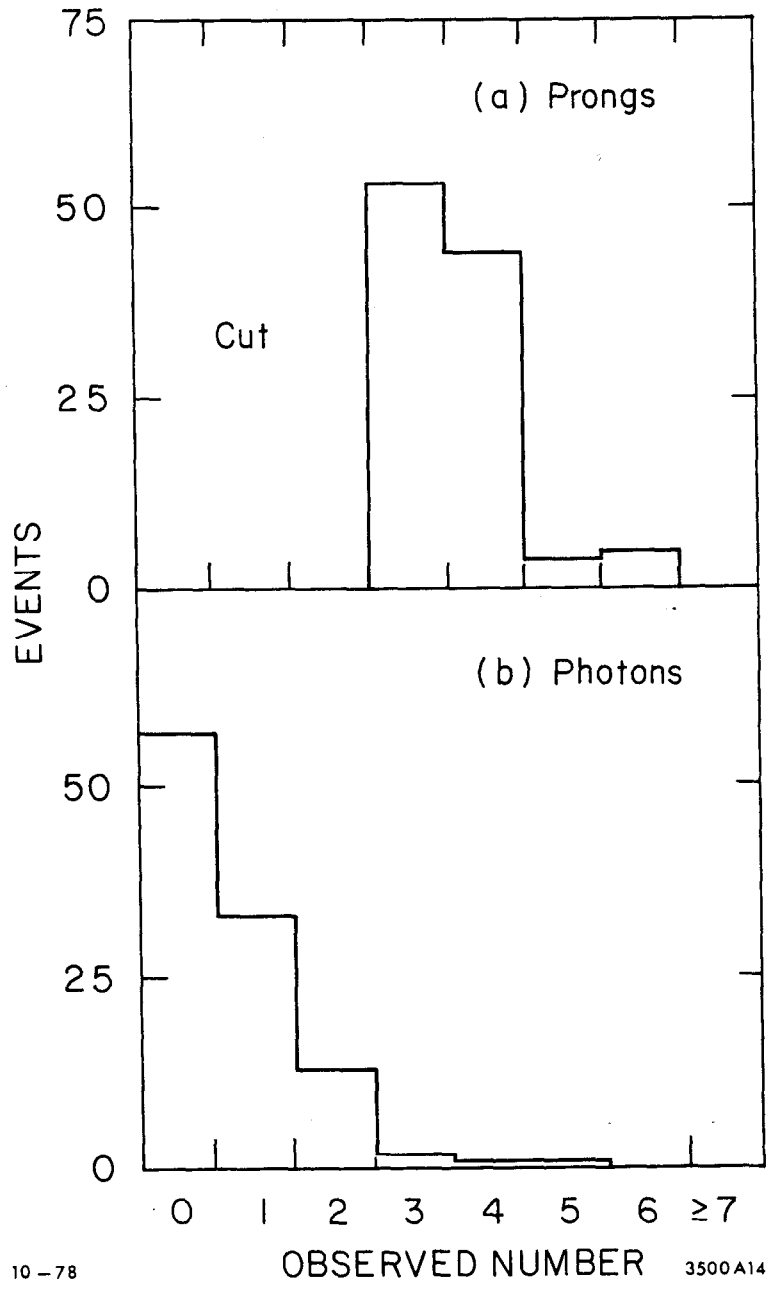

Fig. 18. a) The observed prong distribution of the multiprong electron events in the energy range $3.625 < E_{CM} < 3.72$ GeV (ψ' excluded).

b) The observed photon distribution in the same energy range.

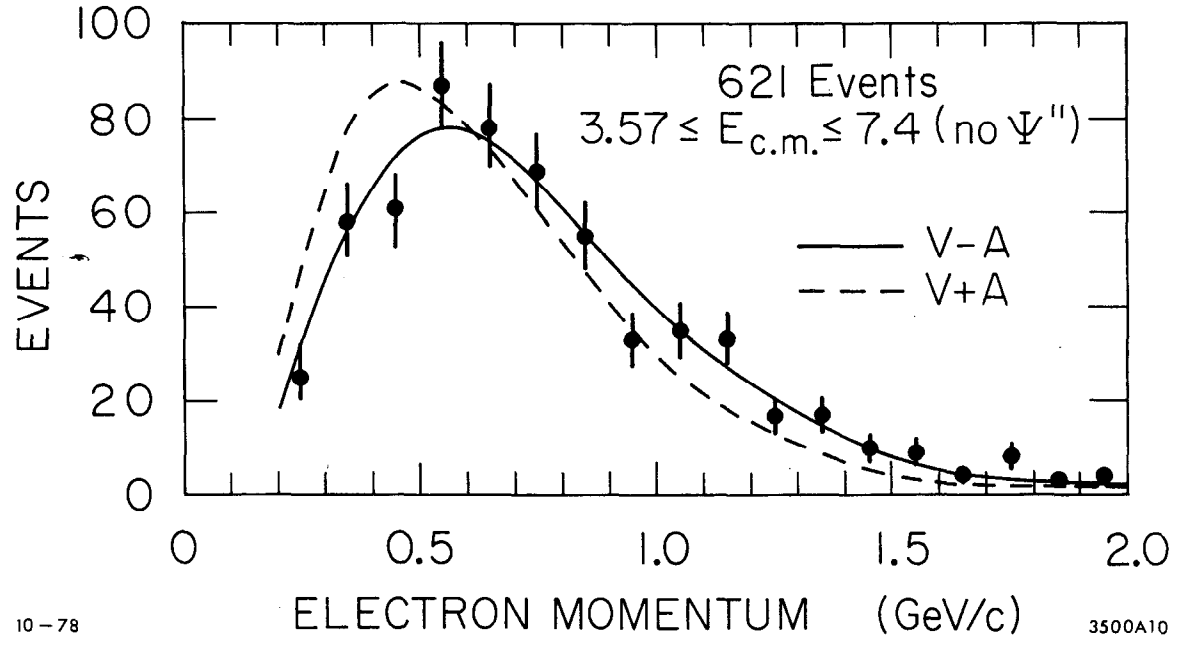

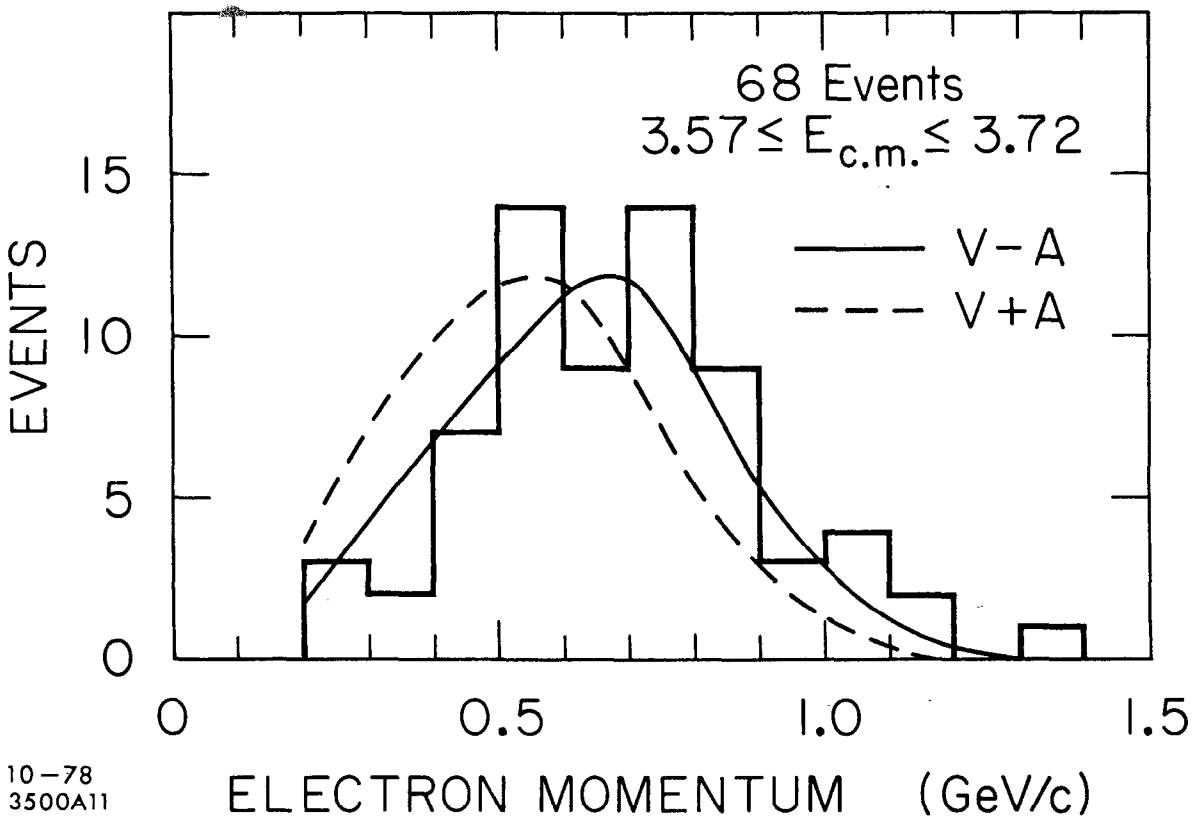

Fig. 19. a) The electron momentum spectrum of the eX events in the range $3.57 \leq E_{CM} \leq 7.4$ GeV after excluding data taken at the ψ''.

b) The spectrum observed below charm threshold in the range $3.57 \leq E_{CM} \leq 3.725$ GeV. The solid (dashed) lines are V-A (V+A) fits with zero ν_τ mass and without radiative corrections. Events with $p_e > 1.0$ GeV/c in spectrum

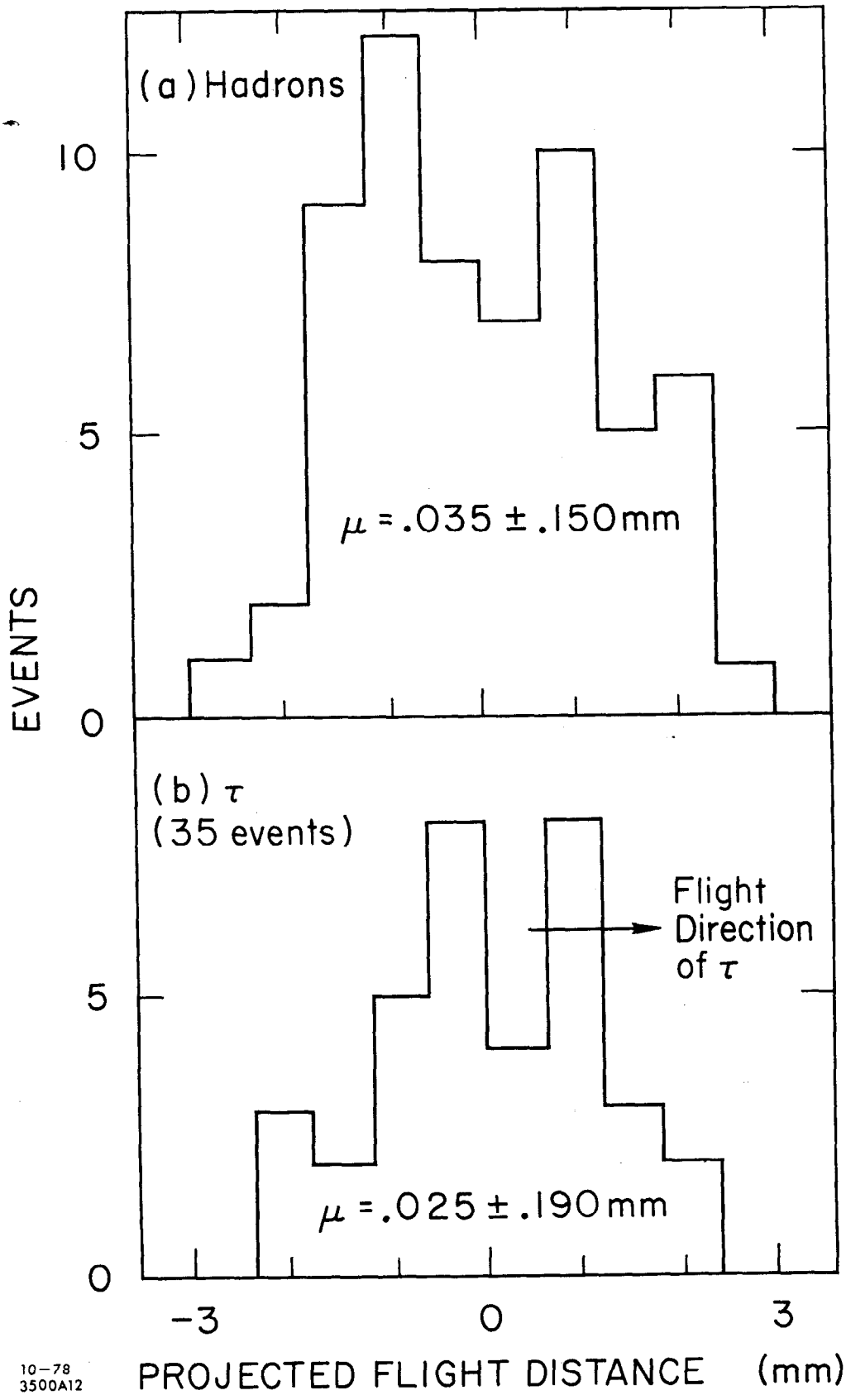

Fig. 20. The projected flight distances using a) a control sample of hadronic events and b) eX events. A measurable τ flight path would lead to a shift in the mean (μ) of the lower distribution in the positive